

**DEVELOPMENT AND DEMONSTRATION OF A STANDARD  
METHODOLOGY FOR RESPIRABLE COAL MINE DUST  
CHARACTERIZATION USING SEM-EDX**

Rachel Mary Sellaro

Thesis submitted to the faculty of Virginia Polytechnic Institute and State University in partial fulfillment of the requirements for the degree of

Master of Science  
In  
Environmental Engineering

Emily A. Sarver, Chair  
Linsey C. Marr  
Nino S. Ripepi

June 10, 2014  
Blacksburg, VA

Keywords: Respirable, Coal Mining, CWP, Silicosis, Dust Exposure, SEM, EDX Spectrum, Characterization, Composition, Size and Shape, Particle

# **DEVELOPMENT AND DEMONSTRATION OF A STANDARD METHODOLOGY FOR RESPIRABLE COAL MINE DUST CHARACTERIZATION USING SEM-EDX**

Rachel Mary Sellaro

## **ABSTRACT**

The purpose of this thesis is to examine the potential for a more comprehensive method of analysis of coal mine dust. Respirable dust is specifically of interest due to its ability to cause occupational lung disease when miners are overexposed to airborne concentrations. A detailed standard methodology to characterize respirable mine dust is carefully investigated with the use of scanning electron microscopy with energy dispersive x-ray (SEM-EDX). In addition to a thorough description of the developed particle level characterization approach, the method is demonstrated with underground respirable dust samples collected from an underground coal mine in Central Appalachia.

Results of this thesis indicate that a comprehensive dust characterization method is possible and can be efficient and effective, when standardized. This analytical approach uses measured compositions, dimensions, and shapes to produce an abundance of data in even a single sample of dust. Verification results show the method is suitable for analysis of respirable particles of common coal mine mineralogy and analysis of many samples in a timely manner. The results obtained from the underground samples in Central Appalachia reveal the quantity of information which can be generated using the developed method. The amount of data which is acquired using the more comprehensive dust characterization method may aid in understanding the health effects of various dust characteristics.

## ACKNOWLEDGEMENTS

First and foremost, I would like to thank my advisor, Dr. Emily Sarver, for all the support and guidance she provided to me throughout my graduate studies. I sincerely appreciate all the time, effort, and advice she gave me, without which I would not have had this wonderful graduate experience.

I would like to thank my committee members, Dr. Linsey Marr and Dr. Nino Ripepi. I am truly lucky to have worked with such distinguished faculty members.

I would also like to thank Steve McCartney and NCFL for help and assistance with all my SEM training and laboratory sessions.

I would also like to thank Dan Baxter for his professional expertise and for all the time and effort he put forth as a consultant in development of the dust characterization method.

A special thanks to the employees of the underground mine in Central Appalachia where I collected my dust samples. I was fortunate to meet and spend my time sampling with some of the most helpful and kind individuals.

Finally, sincere thanks to my parents, Carla and Anthony Sellaro, and my sister, Erica Sellaro, for their encouragement as well as their moral and emotional support over the past two years and throughout my entire life.

## TABLE OF CONTENTS

|   |      |
|---|------|
| List of Figures .....   | vi   |
| List of Tables .....  | viii |
| Preface.....  | ix   |
| Chapter 1: Literature Review .....  | 1    |
| 1. Abstract .....   | 1    |
| 2. Introduction.....  | 1    |
| 3. Dust Generation and Characteristics.....   | 2    |
| 4. Occupational Exposures and Potential Health Impacts .....  | 6    |
| 5. Dust Control.....  | 9    |
| 6. Dust Sampling.....   | 13   |
| 7. Dust Characterization.....   | 16   |
| 8. Conclusions.....   | 18   |
| 9. References.....  | 19   |
| Chapter 2: A Standard Characterization Methodology for Respirable Coal Mine Dust Using SEM-EDX..... | 27   |
| 1. Abstract .....   | 27   |
| 2. Introduction.....  | 27   |
| 3. Description of Developed Dust Characterization Method.....                                       | 28   |
| 3.1 Particle Characteristics of Interest.....   | 28   |
| 3.1.1 Composition.....  | 29   |
| 3.1.2 Dimensions .....  | 35   |
| 3.1.3 Shape, Volume and Mass.....   | 36   |
| 3.2 General Procedures for Dust Characterization .....  | 37   |
| 3.2.1 Sample Collection and Filter Preparation .....  | 38   |

|  |    |
|--|----|
| 3.2.2 Particle Selection and Analysis by SEM-EDX.....  | 39 |
| 3.3 Automated Analysis Program.....  | 42 |
| 4. Preliminary Verification of Developed Characterization Method.....  | 43 |
| 4.1 Materials.....   | 43 |
| 4.2 Results and Discussion.....  | 44 |
| 5. Conclusions.....  | 50 |
| 6. References.....   | 51 |
| Chapter 3: Characterization of Respirable Coal Mine Dust from an Underground Coal Mine in<br>Central Appalachia..... | 54 |
| 1. Abstract.....   | 54 |
| 2. Introduction.....   | 54 |
| 3. Materials and Methods.....  | 57 |
| 4. Results and Discussion.....   | 61 |
| 5. Conclusions.....  | 73 |
| 6. Acknowledgements.....   | 73 |
| 7. References.....   | 73 |
| Chapter 4: Conclusions and Future Work.....  | 77 |
| Appendix A: Chapter 2 Supplemental Data.....   | 79 |

## LIST OF FIGURES

|   |    |
|---|----|
| Figure 2.1. Example spectrum of the PC filter media.....  | 32 |
| Figure 2.2. Comparison of example spectra and images for carbonaceous and alumino-silicate particles at 12,500x magnification.....  | 33 |
| Figure 2.3. Angularity classification categories based on the qualitative analysis of the sharpness of particle edges .....   | 37 |
| Figure 2.4. Example of particle selection and screen shifting via the joystick.....   | 40 |
| Figure 2.5. Illustration of 9 mm diameter filter sub-section and navigation routing for SEM-EDX analysis.....   | 40 |
| Figure 2.6. SEM images at 2,500x magnification for the filter sub-sections from each verification sample showing relative particle densities.....                                     | 44 |
| Figure 2.7. Particle size distribution by number for the Roof Bolter sample .....   | 47 |
| Figure 2.8. Particle size distribution by mass for the Roof Bolter sample .....   | 47 |
| Figure 2.9. Particle size distribution by number for the Belt Drive sample .....  | 48 |
| Figure 2.10. Particle size distribution by mass for the Belt Drive sample.....  | 48 |
| Figure 2.11. Particle size distribution by number for the Intake sample .....   | 49 |
| Figure 2.12. Particle size distribution by mass for the Intake sample .....   | 49 |
| Figure 2.13. Particle compositional distribution by number for the Intake sample, with relative number of particles classified as having angular, transitional or rounded shapes..... | 50 |
| <br>  |    |
| Figure 3.1. Approximated particle densities on each filter subsection. ....   | 63 |
| Figure 3.2. Clockwise from top left, SEM images of the A1, A10, B5, and A8 samples at 2,500x magnification. ....  | 63 |
| Figure 3.3. Composition distributions by number of particles for all twenty-one respirable dust samples.....  | 65 |
| Figure 3.4. Size distributions by number of particles for all respirable dust samples, grouped by similar sample location. ....   | 66 |
| Figure 3.5. Qualitative shape distributions by number of particles for each sample, grouped by similar sample location. ....  | 68 |
| Figure 3.6. Shape distributions by number for each compositional category.....  | 68 |

|   |    |
|---|----|
| Figure 3.7. Size distributions by number for each compositional category.....                                     | 69 |
| Figure 3.8. Estimated mass concentrations and average CPDM mass concentrations for seven Data Set A samples. .... | 71 |
| Figure A.1. Example of a particle classified as mixed carbonaceous.....   | 79 |
| Figure A.2. Example of a particle classified as quartz. ....  | 79 |
| Figure A.3. Example of a particle classified as carbonate.....  | 80 |
| Figure A.4. Example of a particle classified as heavy mineral.....  | 80 |
| Figure A.5. Automated analysis workbook sample information input screen.....                                      | 81 |
| Figure A.6. Automated analysis workbook sample data input screen .....  | 81 |
| Figure A.7. Automated analysis workbook sample output data screen .....   | 81 |
| Figure A.8. Automated analysis workbook size distribution output screen .....                                     | 82 |
| Figure A.9. Automated analysis workbook mass distribution output screen .....                                     | 82 |
| Figure A.10. Automated analysis workbook shape distribution output screen .....                                   | 82 |

## LIST OF TABLES

|   |    |
|---|----|
| Table 1.1. Respirable dust characteristics based on diameter and the percentage of material passing through a size selecting device. .... | 4  |
| Table 1.2. Occupational exposures for continuous mining operations not advancing > 20 feet ...  | 8  |
| Table 2.1. Description of dust categories for particle classification by composition .....  | 31 |
| Table 2.2. Distribution of particle composition by number (and mass) for the method verification samples.....                             | 46 |
| Table 3.1. Dust sample descriptions separated by area or personal sample .....  | 58 |
| Table 3.2. Common minerals and mineral properties represented in each compositional category .....  | 60 |
| Table 3.3 Compositional distributions by number large dust particles observed on Data Set A samples.....                                  | 72 |

## PREFACE

Coal mining generates airborne particulates which can range in size, shape and composition and can remain airborne for extended periods of time. Respirable dust, generally  $< 10 \mu\text{m}$  in size, is hazardous to coal mine workers in elevated concentrations. Although there are regulatory limits set on respirable mass concentrations, many miners are exposed to levels of dust and lung diseases such as CWP and silicosis are still prevalent. Dust samples, collected to demonstrate compliance with regulatory standards, measure mass concentrations of respirable dust as well as crystalline silica content within the samples.

The main objective of this project was to explore a more comprehensive approach to characterizing and analyzing respirable coal mine dust. Scanning electron microscopy with energy dispersive x-ray (SEM-EDX) was employed as the means of analysis. It was essential that the particle-level protocol be time efficient and produce data which allows respirable dust comparisons within and between mines. In completion of these tasks, the aim was to gain knowledge regarding prospective comprehensive characterization of coal dust and advantages resulting in the use of this analytical technique.

This thesis is divided into four main sections. Following the introduction and aims of the report, a literary review summarizes the current information and regulations pertaining to respirable coal mine dust. The review includes the generation and characteristics of dust, occupational exposures and potential health impacts to miners, dust control and sampling techniques, and current and potential dust characterization methods. The second section contains a description as to how the comprehensive characterization method was developed, including a protocol for dust sampling and preparation, standardized particle analysis by SEM-EDX, method validation, and automated data analysis. The third section of this thesis uses real underground respirable dust samples to demonstrate the usefulness of the developed method and the quantity of data which can be accumulated through the characterization process. Trends in dust sample locations regarding composition, size, and shape of particulates are also included. The final section concludes the overall findings of the project and recommends future work for the near and long term.

## **CHAPTER 1: LITERATURE REVIEW**

### **1. Abstract**

The process of mining coal generates dust which may become airborne. Different mining techniques and processes can produce varying dust concentrations and characteristics. Although regulations are set to limit dust concentrations in coal mines, workers are often exposed to respirable dust throughout the workday. Significant health concerns caused by overexposures to dust, such as CWP and silicosis, still affect coal mine workers today, and in specific geographic regions cases of CWP seem to be increasing. Current laws only regulate respirable concentration and silica content within MSHA compliance samples; however a more comprehensive analysis of coal mine dust may be possible with the use of scanning electron microscopy.

### **2. Introduction**

Coal is mined in over 60 countries worldwide, and is expected to remain a significant part of both the global and US energy portfolios for many decades to come (EIA, 2014; EIA: AOE, 2014). In the US, underground coal mines operate throughout the Western, Interior, and Appalachian coal basins, currently employing more than 50,000 mine workers – many of whom may spend their entire career underground. These mines are highly modernized, as advances in technology have supported increased production and efficiency, and exploitation of reserves that were once considered economically unfeasible. Technological development has also allowed underground mining practices and mine environments to grow steadily safer for mine personnel. Nevertheless, occupational injuries and health effects are still a major concern for the coal industry, both in the US and abroad.

With respect to health, respiratory illness is a priority issue for the underground coal sector. Over the past half century, much effort has been aimed at understanding and combating the causes of such illness amongst coal miners. Much has indeed been learned with respect to the influence of dust exposures, and decades of regulation have certainly aided in the protection of miner health. However, there appear to be recent, unexplained increases in respiratory illness

rates among particular groups of miners, which has signaled a need to expand the current understanding of causal factors. Given the fundamental relationship between dust respiration and respiratory disease, one clear direction for research is comprehensive characterization of mine dusts, including particle compositions, shapes and sizes. Though such characteristics are recognized as likely important in terms of respiratory effects, comprehensive characterization of dust particles has heretofore not been a significant focus of research.

This paper broadly reviews dust underground coal mines, including sources, potential health impacts, control strategies, and current analysis methods, and then highlights scanning electron microscopy with energy dispersive x-ray (SEM-EDX) as a potential tool for comprehensive dust characterization.

### **3. Dust Generation and Characteristics**

There are many sources of dust in an underground coal mine. Dust particles are primarily generated when the coal and surrounding rock are broken throughout the mining process. A variety of activities can suspend or re-suspend particles in the air, and the quantity and composition of the dust particles can vary within a mine and between mines depending on the coal seam and host rock characteristics, mining methods, and use of dust suppression systems. Even with proper ventilation underground, constant movement of equipment can create a dust prone atmosphere in which the particles remain airborne for extended periods of time (Potts et al., 1989).

In the US, coal is almost always mined via the room and pillar method using a continuous miner machine or via the longwall method using a longwall miner. These methods are used because they are very efficient due to their high degree of mechanization. However, in other parts of the world, conventional mining (i.e., room and pillar with drill and blast excavation) is still utilized extensively. Considerable dust sources from conventional and continuous mining include cutting, loading, roof bolting, material haulage and handling, transportation, and crushing (Colinet et al., 2010; Organiscak, 1989; Rodgers, 1983). In a longwall operation the principal dust source is the stageloader/crusher, and secondary sources include the intake and belt entries, shearer, and shield advance (Colinet et al., 2010). According to a study done by the US Bureau

of Mines, blasting may account for almost 60% of the total dust generated in a conventional mining section (Organiscak, 1989), but conventional mining may actually produce lower concentrations of dust than continuous and longwall mining methods when comparing mean dust concentrations at the mining face (WHO, 1997). Continuous and longwall mining tend to produce relatively fine products due to the rotational movement of the cutting heads, and thus greater amounts of fine dust (Organiscak, 1989). In longwall mining, the confined space between the active face and the roof supports allows dust to remain in higher concentrations than near the face of a continuous mining section (WHO, 1997).

Mines that use diesel equipment underground can also have a considerable amount of fine diesel particulate matter (DPM), which mixes with the mine dust and remains airborne (Mischler and Colinet, 2009). “Rock dust” can also contribute to higher mineral dust concentrations underground (Colinet and Listak, 2012); this material consists of pulverized inert minerals (e.g., limestone, dolomite, gypsum, etc.) and is commonly applied to floor and wall surfaces in coal mines in order to inhibit explosion propagation.

Dust in the underground mine environment is generally defined as particulate matter with an aerodynamic diameter between about 1-100 micrometers ( $\mu\text{m}$ ). Dust suspended in the air may eventually settle with gravitational forces; however it can remain airborne for an extended period of time depending primarily on its relative and the atmospheric conditions in the mine (ISO, 1995; WHO, 1999). Air velocity in the mining section can greatly affect the rate at which particles settle near or are moved away from a dust source, such as a continuous miner, and velocity is related to both mine ventilation and discreet events (e.g., traffic movement) (Courtney et al., 1986). Under most circumstances, particles that are greater than about 100  $\mu\text{m}$  will not remain suspended for a prolonged length of time, whereas particles in the respirable size range can (WHO, 1999) – and these very small particles are the major concern in the context of occupational health.

Respirable dust is the fraction of suspended particulates that can infiltrate the lungs and is generally considered to have an aerodynamic diameter less than about 10  $\mu\text{m}$  (NIOSH, 1995). As defined by the Mine Safety and Health Administration (MSHA), respirable dust includes particles having the approximate size distribution shown in Table 1.1 (OSHA, 2012). For example, respirable particles with an aerodynamic diameter  $> 2.0 \mu\text{m}$  make up approximately

90% of the total respirable mass and particles < 2.0 μm only contribute to about 10% of the respirable mass. Particles that are slightly larger in size may be inhalable, meaning they can be drawn into the nose or mouth during inhalation, but are less likely to reach the lungs.

*Table 1.1. Respirable dust characteristics based on diameter and the percentage of material passing through a size selecting device.*

| <b>Aerodynamic Diameter (μm)</b> | <b>Respirable Mass (%)</b> |
|----------------------------------|----------------------------|
| 2.0                              | 90                         |
| 2.5                              | 75                         |
| 3.5                              | 50                         |
| 5.0                              | 25                         |
| 10.0                             | 0                          |

Dust that is generated from the coal mining process can have various compositions. It has previously been estimated that respirable coal mine dust is 40 to 95% coal, and the residual portion of the dust consists of minerals such as kaolinite, illite, pyrite, and quartz (NIOSH, 1995), and other constituents including metal oxides, metal sulfides, carbonates, and phosphates (WHO, 1997). These minerals can be ingrained in the coal itself or found in inter-burden material within the coal seam. Perhaps more importantly in some cases, particularly in thin-seam mining operations (i.e., an average coal seam height < 3.6 feet) (Moore et al., 2012), mineral particulates can also be generated when mining necessitates cutting roof and floor material adjacent to the target coal seam (Suarthana et al., 2011; WHO 1997). In the Appalachian region of the US, where thin-seam mining is increasingly common, these particulates may include silica, silicates, and carbonates since the sedimentary layers around coal seams are predominately sandstone and shale (Schatzel, 2006).

In terms of particulates that originate from the coal itself, there is some evidence that dust characteristics may be related to coal “rank”, or formation stage of the coal, because carbon content, volatile matter, mineral content, and moisture within the coal seam can all vary with rank (Landen et al., 2011; WHO, 1997). Some researchers have reported that coal rank may too control particle sizes and shapes produced during the mining process, (Landen et al., 2011; Page and Organiscak, 2002). The physical structure of coal dust itself is often complex and irregular with many concavities, effectively decreasing the specific gravity of particles and dramatically increasing their surface area (vs. more less porous particles). Moisture content of dust < 5 μm is

known to change seasonally (Greninger et al., 1986), which may affect the behavior of the particles or the mass concentration of respirable dust in the mine environment. Prior research has shown that coal dust particles in the 5-10  $\mu\text{m}$  range tend to become increasingly more spherical with decreasing size (Kotrappa, 1972). In this range and at smaller sizes, coal should be substantially liberated from ingrained minerals, so significant “matrix” particles are not expected. However, it is quite possible that very fine (i.e., sub-micron) coal or soft mineral (e.g., silicate) particles may coat larger particles.

Attention to mineral particulates in coal mine dust has been largely focused on crystalline silica due to its known impacts on human health. Recent studies have indicated that silica concentrations in the respirable size range may be elevated when relatively large amounts of floor and roof rock are mined (Organiscak et al., 1990; Joy, 2012). The structure of the rock that contains the silica also has an effect on the amount of respirable silica dust that is generated and the size of the particles (Organiscak et al., 1990). Silica particles can be either pure quartz or quartz coated by other materials, such as clay or coal. If the quartz is coated, then it has a reduced risk of causing harm to mine workers if respired; however pure quartz, also known as free silica, has a greater risk of affecting miners’ health (Grayson, 1991).

Particle sizes and shapes are also important traits that contribute to the hazards of dust inhalation. Dust with an approximate aerodynamic diameter of 2  $\mu\text{m}$  more efficiently deposits in the lungs compared with smaller particles, and larger particles often deposit before reaching the deepest regions of the lungs (WHO, 1999). Shape irregularities (e.g., the surface of silica particles can have very acute shape characteristics) can greatly influence the pathogenesis of respirable dust. For example, a particle considered angular, having a rough surface with many sharp edges, is more likely to reach the deeper lung tissue compared with smoother particles. Additionally, particles less spherical and more fibrotic in shape are more likely to penetrate deeper into the lungs (Hassan and Lau, 2009). Silica can vary dramatically in size. Generally speaking, silica content decreases as particle size decreases (WHO, 1997); however the opposite may be true for continuous miners cutting into significant quantities of roof rock (Organiscak et al., 1990). Although extensive research has been completed regarding exposure to silica dust, other minerals in coal mine dust, such as silicates, have not been widely studied in terms of their impacts on occupational health.

It is important to note that dust metrics are generally considered on a total mass basis by size, as illustrated by the size distribution data shown in Table 1.1 or use of a mass concentration for the federal permissible limit on respirable dust concentration in underground coal mines (i.e., 2 mg/m<sup>3</sup>). While this custom is convenient for analytical measurements and regulatory purposes, and is also used in many other dust-related applications (e.g., NAAQS limits on fine particulates), it does not always allow for a practical understanding of the dust behavior – or health implications of exposure. For example, although two mining sections may have very similar respirable dust concentrations, they may vary significantly in terms of the relative amounts of extremely fine particles, or the mineralogical composition of the dust. Indeed, differences in particulate properties such as specific gravity, surface area, surface charge, and wettability may affect things like settling rate, chemical reactivity and agglomeration. Thus, understanding physical or chemical properties of dust particles, as well as their number concentrations, may be important for assessing occupational exposures and health impacts.

#### **4. Occupational Exposures and Potential Health Impacts**

Coal mine workers may be exposed to respirable dust in almost any location underground, but exposure characteristics such as respirable concentration or silica content may vary significantly with respect to specific work areas, and changing conditions within those areas. Although many underground workers have primary occupations that result in predominate areas of work (e.g., miner operators tend to work at the active face), others are not stationed in one main area throughout the entire shift of each day (e.g., shuttle car drivers, maintenance crew members). Moreover, miners often do not work the same job for their entire tenure underground. Considering all of these factors, determining actual dust exposure characteristics for any individual is not easy.

Prior research on dust exposures in underground coal mines has historically focused on understanding differences in the respirable dust concentration, and more recently great attention has also been given to associated silica content (as a mass percentage). Operators of cutting machines (e.g., continuous miners, longwall miners) typically have the highest dust exposures compared to other face workers (i.e., supply men, laborers, motormen) (WHO, 1997). Longwall mine workers are typically exposed to the highest concentrations of coal dust, due to the high

mining rate within the confined area that the workers occupy. But the levels of respirable silica dust tend to remain relatively low (Parker and Watts, 1987), which may be related to the fact that longwall operations are generally in thicker coal seams. Continuous mining and conventional mining techniques also generate relatively high dust concentrations near the face relative to other areas of the mine, and the respirable dust can often have elevated levels of silica dust (WHO, 1997) – a fact that may be attributable to cutting more rock material with the coal. One study showed, however, that continuous mining can produce up to three times more respirable dust and up to fifteen times more silica dust than conventional mining. Further, the US Bureau of Mines found that respirable dust concentrations in the return increased dramatically when the continuous miner was cutting into roof rock (Organiscak, 1989). Operator technique is also known to affect the rate of dust generation at the cutting face, so individual operators working in similar mine conditions may actually experience different dust exposures (Rodgers, 1983). Although these studies were conducted over two decades ago, the general trends are likely still true today.

Roof bolters may also be exposed to relatively high concentrations of dust, although dust generation near the bolter is not continuous. Instead, instantaneously high concentrations can be produced as the bolter drills directly into the mine roof. Given that roof rock is often shale or sandstone (Organiscak et al., 1990), bolters can also experience elevated silica exposures (WHO, 1997). In addition to dust generated by the bolting process, roof bolters may be exposed to dust generated elsewhere in the mine – which is also the case for a variety of other workers, though bolting often necessitates working fairly close to the active face. Bolters that work on the intake (i.e., clean) air side of a continuous miner have considerably lower dust exposure levels than those working on the return (i.e., exhaust) air side (Tomb et al., 1998). Similarly other mine workers located in intake airways are generally exposed to relatively low respirable dust concentrations, see Table 1.2. An increase in respirable dust around areas of transportation (e.g., shuttle car routes, track and belt entries) and transfer points may also be noticeable due to the frequent movement of vehicles or material (Cronje, 1997).

*Table 1.2. Occupational exposures for continuous mining operations not advancing > 20 feet (Summarized from: Tomb et al., 1998)*

| <b>Occupation</b>                        | <b>Number of Samples</b> | <b>Average Concentration (mg/m<sup>3</sup>)</b> | <b>Percent Greater Than 2.0 mg/m<sup>3</sup></b> |
|--|--------------------------|---|--|
| Continuous Miner Operator                | 350                      | 1.6   | 21   |
| Continuous Miner Helper                  | 142                      | 1.4   | 23   |
| Roof Bolter (intake side)                | 101                      | 1.0   | 7  |
| Roof Bolter (return side)                | 356                      | 1.3   | 18   |
| Roof Bolter Helper                       | 32                       | 1.4   | 22   |
| Section Foreman                          | 40                       | 0.9   | 10   |
| Electrician                              | 20                       | 0.5   | 0  |
| Shuttle Car Operator (standard side)     | 295                      | 0.7   | 5  |
| Shuttle Car Operator (off standard side) | 204                      | 0.8   | 6  |
| Scoop Car Operator                       | 91                       | 0.8   | 8  |
| Motorman                                 | 31                       | 0.4   | 0  |
| Utility Man                              | 62                       | 0.6   | 2  |

Exposure to respirable dust can be harmful to mine workers if particulates reach the lungs, and mine workers have had historically high rates of respiratory diseases in comparison to other occupations (NIOSH, 2008). One of the most common respiratory diseases affecting coal miners is coal workers pneumoconiosis (CWP) (Seixas et al., 1995), which is associated with chronic exposure to respirable dust (Laney et al., 2012). CWP diagnoses range from simple to advanced, with the most critical form being progressive massive fibrosis (PMF). Advanced CWP can lead to reduced lung function, and can often be fatal (Laney et al., 2012). The risk of developing CWP rises with exposure to increasing dust concentrations, and studies suggest that higher coal rank may be associated with greater incidence rates of CWP (Page and Organiscak, 2000). Causal effects of coal rank on respiratory illness have not been studied extensively, however there may be a link between disease incidence and dust particle surface charge, which might allow affect how easily particles deposit in the lungs. The apparent relationship between coal rank and CWP could also be related to mineralogical composition of the dust (Landen et al., 2011).

Another health hazard associated with coal mine dusts is silicosis, which is developed from the respiration of considerable quantities of silica particulates (Page, 2003). Silicosis, one of the

most significant health concerns in the coal industry, can be diagnosed as chronic, accelerated, or acute. Chronic silicosis is the most common type and generally occurs after more than five years of relatively low exposures to silica dust, while accelerated silicosis can arise within about five to ten years of relatively high exposures. The acute form of the disease can develop in just weeks to months of very high silica exposures, and is frequently fatal (NIOSH, 2004). The quantity of silica that causes lung damage can vary; yet the NIOSH recommended exposure limit to respirable crystalline silica, as a TWA for up to a ten hour shift, during a 40-hour work week, is  $0.05 \text{ mg/m}^3$  (NIOSH, 1974).

Other respiratory diseases that have been related to coal mine dust exposure are chronic bronchitis and emphysema. Both can cause shortness of breath and can be deadly if left untreated (Griffiths, 1983). Chronic obstructive pulmonary disease (COPD) and lung cancer have also been associated with exposure to silica dust, as have a variety of non-respiratory diseases such as rheumatoid arthritis, scleroderma, and renal disease (Joy, 2012). In terms of other coal mine dust components, such as metal sulfides (e.g., pyrite), a few recent studies have additionally raised questions as to potential adverse effects on lung function (e.g., Huang et al., 1994, 2005).

Aside from health impacts related to respiration of mine dusts, effects of dust ingestion have also been considered. Given the variety of mineralogical composition and potential reactivity, ingested particles that deposit in the throat, stomach, or other internal organs could be harmful to the human body, although relatively little research has been conducted. Further, dust particles can also accumulate near the eyes and inside the ears and nose. While this produces discomfort, simple contact in these areas is not known to pose a serious health threat (Harrington, 1937).

## **5. Dust Control**

In an effort to help prevent lung disease in mine workers, the Coal Mine Health and Safety Act (CMHSA) of 1969 implemented a federal limit on respirable dust concentrations in underground coal mines. Under CMHSA and the subsequent Federal Mine Safety and Health Act of 1977, the time weighted average (TWA) permissible limit was  $2.0 \text{ mg/m}^3$  over an eight-hour shift (CMHSA, 1969; FMSHA, 1977). On April 23, 2014 the new “dust rule” was published and it goes into effect August 1, 2014. Effective August 1, 2016 the new “dust rule” requires a reduced limit of  $1.5 \text{ mg/m}^3$  for all underground coal mines. The intake air concentration is also

reduced in accordance to the new rule, from 1.0 mg/m<sup>3</sup> to 0.5 mg/m<sup>3</sup> (Federal Register, 2014). If the quartz content in the respirable dust is > 5%, the permissible limit is calculated using the formula shown below in Equation 1.1 (30 CFR Part 70.101). To evidence compliance, mine operators must provide MSHA with dust samples; details regarding dust sampling procedures are discussed below.

$$PEL = \frac{10}{\text{Quartz\% by weight}} \quad (\text{Eq. 1.1})$$

In the 30 years following enactment of CMHSA, surveillance data collected by NIOSH confirms a steady decline in the incidence of lung disease in coal miners across all regions of the US; CWP rates fell from over 11% during the 1970-1974 time period to just 2% during 1995-1999 (CWHSP, 2014; Laney and Attfield, 2014, Laney et al., 2012). However, a unexpected increase in CWP prevalence has been noted over the past decade for young miners (i.e., underground coal miners employed for < 25 years) – and this trend appears to be particularly significant in Central Appalachia, which includes the coalfields of southwestern VA, eastern KY, and southern WV (CDC, 2006; Pollock et al., 2010; Suarhana et al., 2011). Following the 2010 mine disaster at the Upper Big Branch (UBB) Mine, a report by the state medical examiner of WV highlighted this problem: 71% of the deceased miners from which sufficient lung tissue could be analyzed (i.e., 17 out of 24 miners) tested positive for CWP (McAteer and associates, 2011). This is almost ten times the average CWP prevalence rate for WV underground coal miners (i.e., 7.6% according to NIOSH’s 2007 Work-Related Lung Disease Surveillance Report) (NIOSH, 2008). A supplemental study of seven miners from the UBB Mine revealed that six showed evidence of simple CWP, two of which had less than five years experience as an underground coal miner; and one of these young miners also suffered from silicotic nodules, evidence of exposure to significant silica dust (Cohen et al., 2013). The recent uptick in CWP rates has prompted real concern within the industry and regulatory agencies alike, especially for the health of young miners.

Although reductions have been set to limit the exposure of dust to coal mine workers, the National Institute for Occupational Safety and Health (NIOSH) recommends a maximum exposure limit of 1.0 mg/m<sup>3</sup> (NIOSH, 2003). Still, many have questioned whether a reduced

limit would actually target the root problem(s) (e.g., Pollock et al., 2010; Suarthana et al., 2011), since many mines across the US, including Central Appalachia, operate within the current regulatory limit. An important criticism to the reduced respirable dust approach is its unlikeliness to address the potential influence of specific dust characteristics on development of CWP and other lung disease. It has been acknowledged that a relationship between coal seam thickness and lung disease may exist, and may be related to the structure and composition (i.e., mineral content including silica) of the coal and rock layers that are mined, along with the coal rank (Attfield et al., 2011; Laney et al., 2012; Page and Organiscak, 2002) – although there is a clear lack of data on this topic. It should be noted that the new “dust rule” includes changes to respirable dust sampling protocols (i.e., in terms of sampling equipment and duration), but does not change the type or level of dust analysis required. As is currently the case, only respirable dust concentrations (and silica content in applicable samples) are measured.

There are many different strategies for dust suppression and control in underground coal mines, and following enactment of CMHSA there have been substantial improvements in ventilation and mining practices. Water and air are the two primary means of suppressing, diluting, and redirecting dust (Colinet et al., 2010), and it is generally accepted that adequate ventilation, properly maintained equipment, and utilization of advanced mining practices are the first steps to a successful dust control program (Kissell, 2002). Notably, regulatory requirements for dust are focused on engineering controls, not personal protection (NIOSH, 1995) – although many miners do choose to wear respirators and mine operators must make them available (CMHSA, 1969; Harris et al., 2010). MSHA does not require the constant use of respirators due to the obligatory dust reducing techniques that all mines must implement (i.e., engineering controls, training, and dust sampling/monitoring) (NIOSH, 1995).

At the active face where dust concentrations may be the highest, the continuous and longwall miners can utilize water sprays to help reduce respirable dust concentrations around the working face, and this type of suppression, sometimes with the addition of chemical reagents, is the most effective way to prevent large quantities of fugitive dust (Colinet et al., 2010; Kissell, 2002). The type of nozzle, jet pattern, flow, location, and pressure are all factors that can be altered for water sprays depending on the specific dust control plan (Colinet et al., 2010). There are a variety of different reagents that can be added to water sprays. Some chemical reagents include surfactants

such as Surfynol and Mindust, which are used primarily to reduce surface tension on dust particles and improve wettability (Tien and Kim, 1997). Flooded-bed scrubbers are also used to capture airborne dust when the miner head is cutting, and they also help move air toward the face to ventilate and dilute the dust. Furthermore, optimum efficiency scrubbers can remove up to 90% of respirable dust from the air (Colinet et al., 2010). Another way to reduce dust at a continuous mining section is to modify the cutting pattern. For example, less respirable dust is created if the coal seam is mined initially without cutting into any roof rock, and any additional rock that needs to be mined is cut last. This allows the rock dust a greater area to dilute itself (Colinet et al., 2010). This is especially helpful in reducing silica dust. Moreover, face ventilation is regulated by law and is one of the primary methods to reduce respirable dust (Kissell, 2002). With higher velocities of air across the face, dilution is increased, dust is less likely to be transported to other areas, and the risk of dust being trapped in stagnant air areas is reduced. As mentioned previously, areas undergoing active roof bolting are also typically high-dust locations. Roof bolters can utilize a dust collector to facilitate dust removal during the drilling process (Colinet et al., 2010). Common dust collectors utilize a combination of cyclones, a collection bag, and a filter, separating larger particles from the respirable dust and retaining smaller particles inside the collector (Joy et al., 2010).

Proper equipment maintenance throughout the mine can additionally help decrease respirable dust concentrations underground. The bits that are used to cut the coal face can cause more or less dust depending on wear and type. Dull bits that are conical in shape and do not have a carbide tip produce far more dust than newer, unbroken tips with large carbide tip inserts. Fugitive dust from the belt entry can also be controlled with belt maintenance, such as the use of a rotary brush which cleans the belt on the conveying side; wetting of coal during transportation, belt cleaning, and wetting dry belts can also be effective (Colinet et al., 2010). Furthermore, maintenance of diesel equipment can reduce DPM concentrations, and use of water sprays in high traffic areas may limit resuspension of dust in these areas.

## 6. Dust Sampling

Sampling of dust in underground coal mines is primarily done using personal dust samplers. These are generally worn by individuals (i.e., for compliance sampling) and the samples collected are used to determine the mass concentration of respirable dust in the mine atmosphere. Prior to the enactment of the new “dust rule”, samplers are to be in operation for the lesser of either a single working shift or eight hours, according to the Title 30 of the Federal Code of Regulations. In accordance with the new rule, full shift samples should be collected and used for compliance purposes. Personal dust samplers are comprised of a small pump (i.e., Escort ELF type, designated permissible under NIOSH and MSHA) with 10-mm Dorr-Oliver (DO) cyclone, and a pre-weighed 5 mm pore polyvinyl chloride (PVC) filter inside a plastic cassette; the pump is operated at flow rate of about 2.0 L/min (Page et al., 2008), and the cyclone excludes particles larger than the respirable size (i.e., 50% cut size of 4  $\mu\text{m}$ ). These samplers are used for bimonthly sampling of respirable dust acquired from the active working sections of the coal mine.

Following sample collection, the filters are sent to MSHA and analyzed for weight gain and silica content (30 CFR Part 70). Based on Equation 1.2, the TWA respirable dust concentration (i.e. in  $\text{mg}/\text{m}^3$ ) can be computed from the mass of dust on the filter ( $m$ ), the flow rate of the sampling pump ( $V$ ) and the total sampling time ( $t$ ) (Potts et al., 1989). A conversion factor of 1.38 is used to convert to the UK British Medical Research Council (BMRC) criterion (Khan, 2013). The BMRC definition of respirable dust, which relates respirable dust concentrations to worker health effects, uses a different type of sampler to classify dust by particle size; therefore the multiplier converts concentrations, obtained from a personal sampler, to this more universal criterion. Silica content is generally determined by infrared spectroscopy (IR), which is described below. An average of two comparable samples (i.e., one collected by an MSHA inspector and another collected by an operator) is used to determine the amount of silica that is present in the mine dust. This average will determine if the permissible limit on respirable dust is lowered in a specific location of the mine (i.e., using Equation 1.1) (30 CFR Part 70).

$$TWA \text{ Mass Concentration} = \frac{m}{V * t} * 1.38 \quad (\text{Eq. 1.2})$$

While the personal dust sampler has long been used to determine respirable dust concentrations, an inherent flaw in their use for dust control is the fact that measurements cannot be made in real time (i.e., dust concentrations are determined days or even weeks after the dust sample was collected and the exposure occurred). The lapse in time allows for conditional changes in the underground environment (Potts et al., 1989) and, more importantly, this current sampling and characterization approach cannot fully prevent overexposure to silica. Likewise, the current approach to respirable dust analysis does not immediately guard against exposure to high dust concentrations.

The Secretary of Labor and the Federal Advisory Committee on the Elimination of Pneumoconiosis among Coal Mine Workers recommended that NIOSH (Volkwein et al., 2004), in consultation with the coal industry and government, improve upon the available dust sampling devices (Page et al., 2008). The continuous personal dust monitor (CPDM) was developed to provide accurate data at the end of a work shift on an individual worker's respirable dust exposure.

The essential CPDM components include a sampling inlet tube that is fixed adjacent to the miner's cap lamp, HD cyclone, heater, pump, and dust measuring device. This device is a tapered-element oscillating microbalance, which is used to quantify the mass of respirable dust that is deposited on the filter inside the mechanism, and a cumulative exposure mass is indicated on the CPDM display screen (Thermo Scientific, 2009). For engineering purposes, the device also provides quasi real-time exposure data, which allows a user to display a mass concentration based on a user-defined averaging time between 10-60 minutes (Khan, 2013). Having such data easily accessible during the work shift may facilitate miners to modify their environment and respond to changes in the air quality underground (Volkwein et al., 2004).

Study results reported by Volkwein et al. (2004) compared gravimetric filter samplers used in a laboratory setting and in various mine environments to determine the accuracy and precision of the CPDM instrument. The mine samples suggested that the gravimetric sampler and the CPDM results were undistinguishable, and the laboratory results indicated a 95% confidence that CPDM calculations were within  $\pm 25\%$  of the gravimetric samples. It is also noted that when the personal dust monitor is operated at a flow rate of 2.2 L/min, the cyclone better estimates the dust mass (Volkwein et al., 2004) according to the ISO definition of respirable dust (ISO, 1995). According

to Page et al., possible negative bias (i.e., the measured mass concentration is less than the actual mass concentration), with the use of a CPDM, is recognized. This possible loss of dust is assumed to take place between the cyclone exit and the dust sensory zone inside the unit. Also, when comparing CPDM results from samples collected using the same inlet path and a different cyclone (i.e., the Higgins Dewell cyclone) the CPDM mass values were consistently lower compared to results using the original cyclone. Furthermore, prior studies have verified that the CPDM can have a positively induced bias based on heating effects on the filter, in completion of an 8 hour sample. Although bias is generally insignificant, when consecutive low mass measurements are summed, the bias can be noteworthy. Empirical and measurement corrections can be made to reduce the risk of bias during sampling (Page et al., 2008).

Some criticisms of the CPDM include the significant cost of each unit (i.e., about \$13,000) (Thermo Scientific, 2014) and weight (i.e., 6.7 lbs.) (Volkwein et al., 2006), which miners may find cumbersome in their working environment. Additionally, some questions have been raised over the accuracy and precision of the CPDM in terms of detecting the excessive concentration volume (ECV) (Khan, 2013). While MSHA is confident in the evaluation of CPDM variability in calculating the ECV, others have reported that in cases of excessive dust concentrations, levels can go undetected or false measurements can be reported (Khan, 2013).

Although debate over the use of CPDMs for compliance sampling may continue, effective February 1, 2016, the new “dust rule” requires quarterly CPDM samples in lieu of personal dust samples for dust concentration compliance sampling. Improvements in the technology may still be necessary, yet it is clear that this instrument is a powerful tool. Due to the challenges associated with certifying new equipment as permissible for use in coal mines, the CPDM represents significant progress in underground dust monitoring and control. At present, it is the only tool available that can provide any quantification of dust exposures (i.e., as respirable concentration) in the field, although research is currently underway to develop field-based monitoring techniques for some other dust characteristics such as silica content (e.g., see Miller et al., 2012; Miller et al., 2013).

## 7. Dust Characterization

In addition to gravimetric analysis of collected samples (or as an internal function of the CPDM) to determine respirable dust concentrations, other means of dust characterization are also possible and have been used in some instances. As required by regulation, personal dust samples are routinely analyzed for silica. To determine silica content in compliance samples, an infrared spectroscopy (IR) procedure recognized as the P7 analytical method is most commonly used. For this method, a dust sample is analyzed by Fourier transform infrared (FTIR) spectroscopy following ashing of the entire filter on which it was collected (Miller et al., 2012).

X-ray diffraction (XRD) has also been used to determine silica content in coal mine dust samples (Page, 2003). Like IR, XRD allows recognition of raw material in dust samples (Onder and Yigit, 2009), and both techniques are recommended by NIOSH (Page, 2003). In addition to quartz, other elements that may be common in coal mine dust samples including aluminum, silver, calcium, chloride, iron, potassium, magnesium, sodium, sulfur, silicon, and titanium can also be analyzed using XRD (Huggins and Meyers, 1986).

In addition to IR and XRD, a host of other analytical methods could allow for a more in-depth investigation of mine dusts as compared to the routine focus on just two regulated parameters (i.e., respirable dust concentration and silica content.) For example, elemental analysis of dust particles is certainly possible via methods that employ mass spectrometry (MS) to look at digested samples. However, some drawbacks have been noted (e.g., Vassilev and Tascon, 2003; Murphy et al., 2006), including challenges associated with sample preparation, the relatively small number of particles that may be analyzed, and the fact that results do not allow for interpretation of particle mineralogy in samples where a variety of minerals may be present. For coal mine dust samples, specifically, thermogravimetric analysis (TGA) may also be useful in determining mineral to coal ratios. In situations where total mineral content may be of interest, TGA could provide a practical way to screen collected dust samples fairly quickly; but for understanding distribution of mineral types in the samples, additional analysis would be necessary. In terms of particle size distributions of dust, the limitations on equipment that can be used in underground coal mines (i.e., for permissibility) currently rules out the range of typical dust monitors and size analyzers that are currently used for a variety of applications in

atmospheric studies. For particle size (and shape) distributions of collected dust samples, microscopy methods may be used.

While application of several analytical methodologies to separately determine chemical and physical dust characteristics is clearly possible, a comprehensive characterization method capable of determining a range of characteristics at once would be advantageous in terms of efficiency and maintenance of sample integrity. Scanning electron microscopy with energy-dispersive x-ray spectroscopy (SEM-EDX) may be an ideal tool for comprehensive dust characterization. SEM allows the study of individual particles, particularly fine particles (i.e., > 50 nanometers (nm)) and is often used for respirable sized material (Worobiec et al., 2010; Toyoda et al., 2004); transmission electron microscopy (TEM) may be more appropriate for analysis of anything < 1  $\mu\text{m}$  in size (Rice et al., 2013). In addition to the SEM's capability to produce high-resolution images of particles that can be used to determine particle geometries, and thus size and shape distributions for a given sample, the EDX can produce elemental spectra for individual particles, which can be used to determine composition. Unlike some other analytical methods, characterization of particles by SEM-EDX does generally allow for revisiting samples of interest since the method is non-destructive; although, due to the requirement to coat the samples such that they are electrically conductive, pairing with other analytical methods will require coordination and care during sample preparation procedures. Research has shown that large numbers of particles can be characterized in an automated manner (Worobiec et al., 2010), but it should be noted that computer-automated SEM-EDX systems are not widely available. Thus, for characterization of relatively many particles on many samples, a highly standardized methodology must be developed for selection and analysis of individual particles.

SEM has been successfully applied in investigations of environmental aerosols, including particle composition identification (Micheletti et al., 2012; Suzuki, 2006; Kasahara et al., 1993; Kasparian et al., 1998; Carpenter et al., 2002), size and shape classifications (Kasparian et al., 1998; Wang and Luo, 2009), and quantification of particles (Haapala, 1997; Stevens et al., 1993, 1996; Meinander, 1994). SEM-EDX analysis has also been applied to mine dusts, specifically. In the early 1970's SEM was used to explore physical and chemical properties of coal mine dust with the assistance of EDX to identify minerals present in the dust (DeNee, 1972). A more recent

study investigated dust from a mineral mine to assess the mine employee exposure to airborne particulates, and particle size distributions were determined by SEM for dust collected on filters (Terry, 2007). Soot aerosols from the combustion of coal have also been studied using SEM-EDX to determine physical characteristics associated with particle size (Wang and Luo, 2009). In another study aimed at quantifying diesel exhaust emissions in work environments, SEM was utilized to characterize particulate matter (i.e., DPM and other pollutant source particles). In that study, both mass and particle concentrations were explored as well as size distributions of micrometer sized dust. The results indicated that, for DPM, mass concentration of particles < 1  $\mu\text{m}$  in diameter was not indicative of the number concentration of particles; therefore when studying exposure levels, the authors concluded that consideration should be given to number concentrations rather than mass, for nanometer (nm) sized dust (Figler et al., 1996). This is an important point when considering the current mass-based methods for determining and reporting silica content against the possible health implications of very fine silica particles, which may be better assessed on a number basis.

## **8. Conclusions**

Dust generated through the mining process in underground coal mines is a major health concern for workers, and is known to contribute to CWP, silicosis, and other debilitating and potentially fatal lung diseases. Following CMHSA, CWP occurrences have significantly declined in the US, yet rates of CWP amongst young miners appear to be rising in Central Appalachia. The causal factors of these incidences have not yet been confirmed, but specific dust characteristics are likely among them. Thus, determining particle compositions, sizes and shapes, in addition to respirable concentrations, is very important for better understanding and evaluating potential health outcomes associated with dust exposures. More comprehensive dust characterization is certainly possible by a number of methods, and SEM-EDX may be a particularly powerful tool due to its capabilities for simultaneous investigation of a range of particle-level characteristics. However, use of this tool will require development of a standard methodology to ensure that selection and analysis of particles is both statistically sound (i.e., results from selected particles are representative of the entire sample) and efficient (i.e., the time and effort required is practical for routine analysis).

## 9. References

- Attfield, M., Hale, J., et al. (2011). Current Intelligence Bulletin 64: Coal Mine Dust Exposures and Associated Health Outcomes – A Review of Information Published Since 1995. *DHHS (NIOSH)*, Publication No. 2011-172.
- Carpenter, M., Lifshin, E., Gauvin, R. (2002). SEM-EDS Quantative Analysis of Aerosols  $\geq 80$  nm: Impact on Atmospheric Aerosol Characterization Campaigns. *Microscopy and Microanalysis*, 8 (Suppl. 2), 1482CD-1483CD.
- Centers for Disease Control (CDC) (2006). Advanced Cases of Coal Workers' Pneumoconiosis- Two Counties, Virginia. *MMWR*, 55(33).
- Coal Workers' Health Surveillance Program (CWHSP) Data Query System (2014). Occupational Respiratory Disease Surveillance. Available at: <http://webappa.cdc.gov/ords/cwhsp-database.html>.
- Cohen, R., Green, F., Abraham, J., et al. (2013). Coal Mine Dust Lung Disease Among Miners Killed In The Upper Big Branch Disaster - A Systematic Review Of Lung Pathology. *B106. Occupational and Environmental Determinants of Lung Function*, A6063-A6063.
- Colinet, J., Listak, J. (2012). Silica and Respirable Content in Rock Dust Samples. *Coal Age*, 117(12), 48-52.
- Colinet, J., Rider, J., Listak, J., Organiscak, J., Wolfe, A. (2010). Best Practices for Dust Control in Coal Mining. *DHHS (NIOSH)*, Pittsburgh, PA, *IC 9517*, 1-76.
- Courtney, W., Cheng, L., Divers, E. (1986). Deposition of Respirable Coal Dust in an Airway. *US Bureau of Mines Report of Investigations (RI) 9041*.
- Cronje, G., Van Vuuren, P., Rawlins, C. (1997). Respirable Dust in the Intake Airways of a Coal Mine. *Journal of the Mine Ventilation Society of South Africa*, 5(1), 11-14.
- DeNee, P. (1972). Mine dust characterization using the scanning electron microscope. *American Industrial Hygiene Association Journal*, 33(10), 654-660.
- EIA (2014). *International Energy Statistics: Coal*. Retrieved from U.S. Energy Information Administration database.
- EIA: AOE (2014). *Annual Energy Outlook 2014 Early Release Overview*. Retrieved from U.S. Energy Information Administration website.

Federal Coal Mine Health and Safety Act (CMHSA) (1969). Public Law no. 91-173.

Federal Mine Safety and Health Act (FMSHA) (1977). Public Law no. 91-173, as amended by Public Law no. 95-164

Federal Register (2014). Lowering Miner's Exposure to Respirable Coal Mine Dust, Including Continuous Personal Dust Monitors. *79 Fed. Reg.* 24813.

Figler, B., Sahle, W., Krantz, S., Ulfvarson, U. (1996). Diesel Exhaust Quantification by Scanning Electron Microscope with Special Emphasis on Particle Size Distribution. *The Science of the Total Environment*, 193, 77-83.

Grayson, R. (1991). Potential Role of Particle Characteristics on Coal Mine Respirable Dust Standards. SME, *Mining Engineering*, 1991.

Greninger, N., Courtney, W., Divers, E. (1986). Season Variation in Respirable Dust Concentration in U.S. Coal Mines. *US Bureau of Mines Report of Investigations (RI) 9014*.

Griffiths, R. (1983). Occupational Health Effects of Airborne Coal Dust and Mine Gas. AUSIMM, Illawarra Branch Symposium, Ventilation of Coal Mines.

Haapala, H. (1997). The Use of SEM/EDX for Studying the Distribution of Air Pollutants in the Surroundings of the Emission Source. *Environmental Pollution*, 9, 361-363.

Harrington, D. (1937). Dust Hazards and their Control in Mining. *US Bureau of Mines Report of Investigations (RI) 6954*.

Harris, H., DeSieghardt, W., Burgess, W., Reist, P. (2010). Respirator Usage and Effectiveness in Bituminous Coal Mining Operations. *American Industrial Hygiene Association Journal*, 35(3), 159-164.

Hassan, M., and Lau, R., (2009). Effect of particle shape on dry particle inhalation: study of flowability, aerosolization, and deposition properties. *AAPS PharmSciTech*, 10(4), 1252-1262.

Huang, X., Li, W., Attfield, M., et al. (2005). Mapping and Prediction of Coal Workers' Pneumoconiosis with Bioavailable Iron Content in the Bituminous Coals. *Environmental Health Perspective*, 113(8), 964-968.

Huang, X., Zalma, R., Pezerat, H. (1994). Factors that Influence the Formation and Stability of Hydrated Ferrous Sulfate in Coal Dust, Possible Relation to the Emphysema of Coal Miners. *Chemical Research in Toxicology*, 7, 451-457.

- Huggins, C., Meyers, G. (1986). Particle Size Distribution of Quartz and Other Respirable Dust Particles Collected at Metal Mines, Nonmetal Mines, and Processing Plants. *US Bureau of Mines Report of Investigations (RI) 9053*.
- ISO (1995). *Air quality-particle size fraction definitions for health related sampling, ISO Standard 7708*. International Organization for Standardization (ISO), Geneva.
- Joy, G. (2012). Evaluation of the Approach to Respirable Quartz Exposure Control in U.S. Coal Mines. *Journal of Occupational Environmental Hygiene*, 9(2), 65-68.
- Joy, G., Beck, T., Listak, J. (2010). Respirable Quartz Hazard Associated with Coal Mine Roof Bolter Dust. *NIOSH*, Pittsburgh, PA.
- Kasahara, M., Shinoda, K., Yoshida, K., Takahashi, K. (1993). Characterization of Atmospheric Aerosol based on SEM-EDX Analysis of Individual Particles. *Journal of Aerosol Science*, 24(Suppl. 1), S585-S586.
- Kasparian, J., Frejafon, E., Rambaldi, P., et al. (1998). Characterization of Urban Aerosols using SEM-Microscopy, X-ray Analysis and Lidar Measurements. *Atmospheric Environment*, 32(17), 2957-2967.
- Khan, A. (2013). Characterizing the Variability in Respirable Dust Exposure using Johnson Transformtaion and Re-examining 2010 Proposed Changes to the U.S. Underground Coal Mine Dust Standard, University of Kentucky. Theses and Dissertations-Mining Engineering, Paper 5.
- Kissell, F., Volkwein, J., Kohler, J. (2002). Historical Perspective of Personal Dust Sampling in Coal Mines. Mine Ventilation Conference, Lisse, Netherlands: AA Balkema, 619-623.
- Kotrappa, P. (1972). Shape Factors for Aerosols of Coal, UO<sub>2</sub>, and TiO<sub>2</sub> in Respirable Size Range, Assessment of Airborne Particles. Proceedings of the 3<sup>rd</sup> Rochester International Conference on Environmental Toxicity, Rochester, NY, 331-358.
- Landen, D., Wassel, A., McWilliams, L., Patel, J. (2011). Coal Dust Exposure and Mortality from Ischemic Heart Disease among a Cohort of U.S. Coal Miners. *American Journal of Industrial Medicine*, 54(10), 727-733.
- Laney, A., Attfield, M. (2014). Examination of Potential Sources of Bias in the US Coal Workers' Health Surveillance Program. *American Journal of Public Health*, 104(1), 165-170.

- Laney, A., Wolfe, A., Petsonk, E., Halldin, C. (2012). Pneumoconiosis and Advanced Occupational Lung Disease among Surface Coal Miners – 16 States, 2012-2011. *MMWR*, 61(23), 431-434.
- Mandatory Health Standards – Underground Coal Mines, 30 CFR Part 70, (1994).
- McAteer J.D. and associates (2011). Upper Big Branch Report to the Governor. Governor's Independent Investigation Panel, May 2011.
- Meinander, O. (1994). Eestin palavan kiven päästöistä aiheutuvan hiukkaslaskeuman koostumus, (The Composition of the Particle Deposition from the Emissions of the Oil-shale Energy Plants in Estonia). Ilmatieteen laitos, Ilmanlaatuosasto, Helsinki.
- Micheletti, M., Murrini, L., Debray, M., et al. (2012). Elemental Analysis of Aerosols Collected at the Pierre Auger Cosmic Ray Observatory with PIXE Technique Complemented with SEM/EDX. *Nuclear Instruments and Methods in Physics Research*, B288, 10-17.
- Miller, A., Drake, P., Murphy, N., et al. (2013). Deposition Uniformity of Coal Dust on Filters and Its Effects on the Accuracy of FTIR Analyses for Silica. *Aerosol Science and Technology*, 47, 724-733.
- Miller, A., Drake, P., Murphy, N., Noll, J., Volkwein, J. (2012). Evaluating Portable Infrared Spectrometers for Measuring the Silica Content of Coal Dust. *Journal of Environmental Monitoring*, 14, 48-55.
- Mischler, S., Colinet, J. (2009). Controlling and Monitoring Diesel Emissions in Underground Mines in the United States, Mine Ventilation. Proceedings of the Ninth International Mine Ventilation Congress, New Delhi, India, 879-888.
- Moore, S., Pollard, J., Nelson, M. (2012). Task-specific Postures in Low-seam Underground Coal Mining. *International Journal of Industrial Ergonomics*, 42(2), 241-248.
- Murphy, D., Cziczo, D., Froyd, K., et al. (2006). Single-particle Mass Spectrometry of Tropospheric Aerosol Particles. *Journal of Geophysical Research*, 111, D23S32.
- National Institute for Occupational Safety and Health (1974). Criteria for a Recommended Standard – Occupational Exposure to Crystalline Silica. *DHEW (NIOSH)*, Publication No. 75-120.

National Institute for Occupational Safety and Health (1995). Criteria for a Recommended Standard, Occupational Exposure to Respirable Coal Mine Dust. *DHHS (NIOSH)*, Publication No. 95-106.

National Institute for Occupational Safety and Health (2003). Work-Related Lung Disease Surveillance Report, 2002. *DDHS (NIOSH)*, Publication No. 2003-2111.

National Institute for Occupational Safety and Health (2004). Silicosis: Learn the Facts. *DDHS (NIOSH)*, Publication No. 2004-2108.

National Institute for Occupational Safety and Health (2008). Work-Related Lung Disease Surveillance Report, 2007. *DHHS (NIOSH)*, Publication No. 2008-2143a.

Occupational Health and Safety Administration (OSHA) (2014). Chapter 1: Dust and Its Control. US Department of Labor, Available at: [https://www.osha.gov/dsg/topics/silicacrystalline/dust/chapter\\_1.html](https://www.osha.gov/dsg/topics/silicacrystalline/dust/chapter_1.html).

Onder, M., Yigit, E. (2009). Assessment of Respirable Dust Exposures in an Opencast Coal Mine. *Environmental Monitoring Assessment*, 152, 393-401.

Organiscak, J. (1989). Respirable Dust Generation: Comparison of Continuous and Conventional Mining Methods When Excavating Rock in Coal Mines. *US Bureau of Mines Report of Investigations (RI) 9233*.

Organiscak, J., Page, S., Jankowski, R. (1990). Sources and Characteristics of Quartz Dust in Coal Mines. *US Bureau of Mines Report of Investigations (RI) 9271*.

Page, S. (2003). Comparison of Coal Mine Dust Size Distributions and Calibration Standards for Crystalline Silica Analysis. *American Industrial Hygiene Association Journal*, 64(1), 30-39.

Page, S., Organiscak, J. (2000). Suggestion of a Cause- and-Effect Relationship among Coal Rank, Airborne Dust, and Incidence of Workers' Pneumoconiosis. *American Industrial Hygiene Association Journal*, 61(6), 785-787.

Page, S., Organiscak, J. (2002). Using Proximate Analysis to Characterize Airborne Dust Generation from Bituminous Coals. *Aerosol Science and Technology*, 36(6), 721-733.

Page, S., Volkwein, J., Vinson, R., et al. (2008). Equivalency of a Personal Dust Monitor to the Current United States Coal Mine Respirable Dust Sampler. *Journal of Environmental Monitoring*, 10(1), 96-101.

- Parker, D., Watts, W. (1987). Respirable Dust Levels in Coal, Metal, and Nonmetal Mines. *US Bureau of Mines Report of Investigations* (RI) 9125.
- Pollock, D., Potts, J., Joy, G. (2010). Investigation into Dust Exposures and Mining Practices in Mines in the Southern Appalachian Region. *Mining Engineering*, 62(2), 44-49.
- Potts, D., Jankowski, R., Niewiadomski, G. (1989). Respirable Dust Sources and Controls on Continuous Auger Mining Sections. *US Bureau of Mines Report of Investigations* (RI) 9223.
- Respirable Dust Standard when Quartz is Present, 30 CFR Part 70.101, (1994).
- Rice, S., Chan, C., Brown, S., et al. (2013). Particle Size Distributions by Transmission Electron Microscopy: an Interlaboratory Comparison Case Study. *Metrologia*, 50(6), 663-678.
- Rodgers, S. (1983). Evaluation of Dust Sources and Control Techniques for Conventional Mining. Vol. 1 - Field Studies. *US Bureau of Mines*, Mining Research Contract Report, *OFR*, 5(1), MSAR 83-59.
- Schatzel, S. (2006). Characterization of Source Rocks Producing Respirable Quartz and Aluminosilicate Dust in Underground US Coal Mines. Proceedings of the 23<sup>rd</sup> Annual International Pittsburgh Coal Conference, University of Pittsburgh, School of Engineering, Pittsburgh, PA, 38-39.
- Seixas, N., Hewett, P., Robins, T., Haney, R. (1995). Variability of Particle Size-Specific Fractions of Personal Coal Mine Dust Exposures. *American Industrial Hygiene Association Journal*, 56(3), 243.
- Stevens, R., Pinto, J., Mamane, Y., et al. (1993). Chemical and Physical Properties of Emissions from Kuwaiti Oil Fires. *Water Science and Technology*, 27, 223-233.
- Stevens, R., Pinto, J., Mamane, Y., Willis, R. (1996). Characterization and Source Apportionment of Particulate Matter in the Czech Republic. *Journal of Aerosol Science*, 27(1), S685-S686.
- Suarthana, E., Laney, A., Storey, E., et al. (2011). Coal workers' pneumoconiosis in the United States: regional differences 40 years after implementation of the 1969 Federal Coal Mine Health and Safety Act. *Occupational Environmental Medicine*, 68, 908-913.
- Suzuki, K. (2006). Characterisation of Airborne Particulates and Associated Trace Metals Deposited on Tree Bark by ICP-OES, ICP-MS, SEM-EDX, and Laser Ablation ICP-MS. *Atmospheric Environment*, 40, 2626-2634.

- Terry, K. (2007). Particle Size Distribution of Airborne Dusts Using a Scanning Electron Microscope. *Aerosol Science and Technology*, 23(3), 475-478.
- Thermo Scientific (2009). *Thermo Scientific PDM3600 Personal Dust Monitor*, Retrieved from [http://www.thermo.com/eThermo/CMA/PDFs/Various/File\\_52082.pdf](http://www.thermo.com/eThermo/CMA/PDFs/Various/File_52082.pdf)
- Thermo Scientific (2014). Thermo Fisher Scientific Inc., *PDM3600*, Retrieved from Thermo Scientific Price Quote.
- Tien, J., Kim, J. (1997). Respirable Coal Dust Control Using Surfactants. *Applied Occupational and Environmental Hygiene*, 12(12), 957-963.
- Tomb, T., Peluso, R., Gero, A., Seiler, J. (1998). Study to Assess Respirable Dust Exposures in Underground US Coal Mines. *Applied Occupational Environmental Hygiene*, 13(1), 62-72.
- Toyoda, M., Kaibuchi, K., Nagasono, M., et al. (2004). X-ray Analysis of a Single Aerosol Particle with Combination of Scanning Electron Microscope and Synchrotron Radiation X-ray Microscope. *Spectrochimica Acta Part B*, 59, 1311-1315.
- Vassilev, S., Tascon, J. (2003). Methods for Characterization of Inorganic and Mineral Matter in Coal: A Critical Overview. *Energy and Fuels*, 17, 271-281.
- Volkwein, J., Vinson, R., McWilliams, L., et al. (2004). Performance of a New Personal Respirable Dust Monitor for Mine Use. U.S. Department of Health and Human Services, *CDC, Report of Investigations* (RI) 9663, Pittsburgh, PA.
- Volkwein, J., Vinson, R., Page, S., et al. (2006). Laboratory and Field Performance of a Continuously Measuring Personal Respirable Dust Monitor. U.S. Department of Health and Human Services, *CDC, Report of Investigations* (RI) 9669, Pittsburgh, PA.
- Wang, A., Luo, B. (2009). Application SEM to Analysis Formation Characteristic of Soot Aerosol Emitted from Lump-Coal Combustion in Fixed-Bed. Proceedings of the Power and Energy Engineering Conference, APPEEC, Asia-Pacific.
- WHO (1997). Silica, some Silicates, Coal Dust and Para-aramid Fibrils. *World Health Organization (WHO)*, International Agency for Research on Cancer (IRAC), 68.
- WHO (1999). Hazard Prevention and Control in the Work Environment: Airborne Dust. *World Health Organization (WHO)*, Occupational and Environmental Health: Department of Protection of the Human Environment, Geneva, 99.14.

Worobiec, A., Potgieter-Vermaak, S., Brooker, A., et al. (2010). Interfaced SEM/EDX and Micro-Raman Spectrometry for Characterisation of Heterogeneous Environmental Particles – Fundamental and Practical Challenges. *Microchemical Journal*, 94, 65-72.

## **CHAPTER 2: A STANDARD CHARACTERIZATION METHODOLOGY FOR RESPIRABLE COAL MINE DUST USING SEM-EDX**

### **1. Abstract**

Coal miners can be exposed to a variety of dust characteristics depending on their work activities, and some exposures may put miners at risk for serious lung diseases like CWP and silicosis. Regulations have been placed on the total mass concentration of respirable dust allowable in working areas of an underground coal mine, and also the silica mass content of respirable dust. However, relatively little emphasis has been placed on other characteristics of dust exposures that may also be important in terms of occupational health, such as the compositional, size, and shape distributions of respirable particles. Currently a standard methodology does not exist to complete a more comprehensive particle-level analysis of respirable dust from coal mines. This paper describes such a method using Scanning Electron Microscopy (SEM) and Energy Dispersive X-ray (EDX), and its preliminary verification based on analysis of three respirable dust samples collected from an underground mine in Central Appalachia.

### **2. Introduction**

Coal mine dust has long been linked to various lung diseases like coal workers pneumoconiosis (CWP) and silicosis (Laney et al., 2012; Attfield et al., 2011). Implementation of dust regulations in the US beginning in the late 1960s has significantly decreased overall incidence of such diseases over the past several decades, (CWHSP, 2014; Laney et al., 2012; Suarathana et al., 2011) but analysis of long-term surveillance data appears to show a recent and unexpected uptick in disease amongst some miners in particular geographic regions like Central Appalachia (CWHSP, 2014; Laney and Attfield, 2014; CDC, 2006; Pollock et al., 2010). Such trends are alarming considering that most coal mines currently operate below regulatory limits on respirable dust (i.e., particulates with aerodynamic diameter  $<10\ \mu\text{m}$ ), which generally pertain to total mass concentration and crystalline silica content. These trends may suggest that other exposure factors, including specific dust characteristics such as particle composition, size and shape distributions, may be important in the occupational health context. While MSHA's new

dust rule<sup>1</sup> issued in April 2014 targets further reductions in respirable dust concentrations, it is unclear if or how the lowered limits will affect health outcomes for miners in locations where causal factors for disease are not well understood. Indeed, more comprehensive characterization of coal mine dust is necessary to fully explore these factors.

Currently, a standard methodology for comprehensive, particle-level characterization of coal mine dusts does not exist. This paper describes such a methodology, which uses scanning electron microscopy equipped with energy dispersive x-ray (SEM-EDX). A major objective of the method development included optimization of manual analytical efforts – i.e., minimizing the required SEM user time for each sample, while maximizing the range of valuable raw data types to be collected. The developed method includes particle-level analysis of composition, size and shape, from which mass and volume can also be estimated. Construction of automated spreadsheet program for computational analysis is also described here, as well as preliminary verification of the dust characterization method using three samples collected in the field.

### **3. Description of Developed Dust Characterization Method**

The following sections provide a detailed discussion of the particle characteristics that are included in the developed dust characterization method, as well as a description of procedures used for dust sample collection and preparation, and selection and analysis of specific particles by SEM-EDX. Additionally, computation via an automated analysis program is described for easy analysis of raw data inputs.

#### ***3.1 Particle Characteristics of Interest***

To fully characterize particles, specific properties are of interest. Particle composition, dimensions, and shape are values which are determined with SEM-EDX, and volume and mass

---

<sup>1</sup> The “new dust rule” was first proposed by the US Mine Safety and Health Administration (MSHA) on October 19, 2010 and was finally issued under the title *Lowering Miners' Exposure to Respirable Coal Mine Dust Including Continuous Personal Dust Monitors* on April 23, 2014 (Federal Register, 2014). The rule makes a number of changes to previous regulations on dust limits and sampling in underground coal mines, and specifically will reduce the permissible respirable dust concentration from 2.0 to 1.5 mg/m<sup>3</sup>. It will also require use of continuous personal dust monitors (CPDMs) by mine operators, and require that citations be issued in any instances where MSHA-collected samples for single, full shifts exceed the new 1.5 mg/m<sup>3</sup> limit.

are calculated as a result of the analysis. These particle characteristics provide an abundance of data and information regarding respirable dust samples and aid in the comprehensive analysis of coal mine dust.

### 3.1.1 Composition

Classification of the dust particles is based on their EDX spectra, which provides a graphical representation of the elements associated with the particle surface. The spectra are generated by detection of x-ray emissions from the particle, caused by interaction of the SEM electron beam with its surface; each element on the particle surface produces a characteristic x-ray when excited by the impinging electrons. Each peak of a spectrum thus represents a specific element, and relationships between peak heights can provide some indication of the elemental composition (i.e., minerals can be identified by their atomic stoichiometry). For relatively small particles, such as respirable dust particulates, the electrons may penetrate deep enough into the particle (e.g., to a depth of about 1 $\mu$ m) to provide relatively good information about its overall composition.

For the developed dust characterization method, considerable effort was aimed at establishing a set of pre-determined compositional categories into most particles in a coal mine dust sample would be expected to fit. In order to do this, lab-generated dust samples were collected as a part of method development using run-of-mine (ROM) coal, consisting of coal and rock (i.e., primarily shale and sandstone) taken from an underground coal mine in Central Appalachia. The mine is considered “low seam” based on its average coal seam thickness of 24 inches. With an average extraction height of 40 inches, the operation is thus cutting about 16 inches of roof and floor rock during coal extraction. Dust was generated under a laboratory fume hood by pulverizing a representative sample multiple times, using a fine-material pulverizer which was cleaned prior to use, split from the ROM. For each dust sample collected, a pump was operated at a flow rate of 5 L/min to collect dust onto a 37- mm diameter polycarbonate (PC) filter (0.4  $\mu$ m pore size), which was positioned near the top of the fume hood, just below the suction fan; this arrangement was deemed appropriate to collect relatively fine dust over short time periods (i.e., 5-10 minutes) without the use of a cyclone or other size classifier. A cyclone was not used to collect the laboratory samples, since the primary purposes of these samples were determination of the ROM mineralogy (i.e., such that appropriate particle composition categories

could be identified) and development of standard procedures to be used during the SEM-EDX analysis. For more in-depth investigation of mineralogy, dust samples were also generated by pulverizing approximately pure rock and pure coal sub-samples hand-picked from the ROM.

An FEI Quanta 600 FEG environmental scanning electron microscope (ESEM) equipped with a Bruker Quantax 400 EDX spectroscope was employed. In conjunction with the SEM-EDX hardware, image analysis software which comes standard with the FEI model (FEI, Hillsboro, OR) and Esprit software (Bruker, Ewing, NJ) provided imaging and graphical spectra results. The ESEM was operated under high vacuum at 15 kV with a 5.0 spot size and a working distance of approximately 12-13 mm, which was observed to be optimal for this particular scope and application. To prepare collected dust samples for SEM-EDX analysis, filters were removed with clean tweezers, and on a clean, hard surface, a 9-mm diameter trephine (i.e., a cylindrical blade) and a clean razorblade were used to extract the center of the filter. The center sub-section was then attached to an SEM pin-stub mount with double-sided copper tape and sputter coated with gold/palladium (Au/Pd) to generate a thickness of about 10-20 nm (i.e., 60-second sputtering time) and create the conductive surface layer needed for electron microscopy analysis.

Based on observed mineralogy of the lab-generated ROM dust samples, it was determined that twelve elemental peaks should be included in the developed coal mine dust characterization methodology: carbon, oxygen, sodium, magnesium, aluminum, silicon, sulfur, potassium, calcium, titanium, iron, and copper. Further, it was determined that most particles could be classified into six defined categories based on the peak height ratios: “carbonaceous,” “mixed carbonaceous,” “alumino-silicate,” “quartz,” “carbonate,” and “heavy mineral.” Although the ROM dust samples did not contain significant carbonate particles, due to rock dusting throughout the mine (i.e., applying pulverized inert minerals, such as limestone or dolomite, to coal and rock surfaces underground in order to reduce explosion propagation), carbonate particles are likely to be collected in field samples. For the relatively few particles that could not be classified into one of these six categories, a seventh category “other” was created.

Table 2.1 provides examples of typical minerals associated with coal mine dust that fall into each of these categories, and defines the rules developed for compositional classification. These rules are fundamentally based on atomic abundance (i.e., atomic percentage equivalencies of primary minerals in each category), which are correlated to the real-time observed peak height

ratios (i.e., Cps/eV) on EDX spectra of specific elements for each category. For the purpose of expedient decision making during SEM-EDX use, the observed peak heights are the main parameters used for characterization.

*Table 2.1. Description of dust categories for particle classification by composition*

| <b>Dust Category</b> | <b>Example Mineralogy</b>           | <b>Parameters for Classification (Atomic % Equivalent)</b>                               | <b>Real Time Classification (Raw Peak Heights (Cps/eV))</b>                            |
|----------------------|-------------------------------------|--|--|
| Carbonaceous         | Coal                                | <i>Carbon</i> ≥70%<br>Oxygen ≤30%  | <i>Carbon</i> ≥80<br>Oxygen ≤20  |
| Mixed Carbonaceous   | Biogenic/Organic Carbonaceous Clays | <i>Silicon</i> ≥2%, <4%<br><i>Aluminum</i> ≥2%, <4%<br><i>Carbon</i> >70%<br>Oxygen <20% | <i>Silicon</i> ≥10, <20<br><i>Aluminum</i> ≥10, <20<br><i>Carbon</i> ≥80<br>Oxygen ≤20 |
| Alumino-silicate     | Clays, Feldspars                    | <i>Silicon</i> ≥4%<br><i>Aluminum</i> ≥3%<br>Oxygen >20%                                 | <i>Silicon</i> ≥20<br><i>Aluminum</i> ≥20<br>Oxygen >20                                |
| Quartz               | Crystalline Silica                  | <i>Silicon</i> ≥5%<br>Oxygen >20%  | <i>Silicon</i> ≥20<br>Oxygen >20   |
| Carbonate            | Rock Dust, Calcite, Dolomite        | <i>Calcium/Magnesium</i> ≥5%<br>Oxygen >20%<br>Carbon <70%                               | <i>Calcium/Magnesium</i> ≥20<br>Oxygen >20<br>Carbon <80                               |
| Heavy Mineral        | Pyrite, Titanium Oxides             | <i>Iron/Titanium/Aluminum</i> ≥5%<br>Oxygen >20%   | <i>Iron/Titanium/Aluminum</i> ≥20<br>Oxygen >20  |
| Other                | DPM, etc.                           | Does not fit above conditions  | Does not fit above conditions  |

\*DE- Dominant element(s) are italicized for each defined category<sup>2</sup>

Each of the six defined categories has one or more dominant elements (DEs) which must exceed a minimum atomic percentage (or peak height) for a particle to be classified into that category. These minimums are based on the authors' SEM experience with particles in the respirable size range, but it is recognized that particles in this range often produce spectra that

<sup>2</sup> For particles < 1.5 μm in long dimension, DE content can be up to 50% less than the values noted in Table 2.1 for all defined groups with the exception of "carbonaceous". It was found that the filter media increasingly influences the spectra of smaller particles, with carbon content increasing and DE content decreasing (see below for details).

are influenced by electron penetration depth and/or electron scattering (Laskin and Cowin, 2001). Electron penetration depth is generally defined as the depth at which the electron beam can penetrate the sample material. Thus, particles that are very small or thin may produce x-ray spectra that are greatly affected by filter background; and since the developed methodology for dust characterization utilizes PC filters, small particles or those with significant penetration depth are generally known to exhibit apparently high carbon abundances.

Figure 2.1 shows the spectrum for a PC filter, which has atomic percentage equivalencies of approximately 85% carbon and 15% oxygen, and Figure 2.2 shows spectra and actual SEM images of typical “carbonaceous” and “alumino-silicate” particles. (See Appendix A, Figures A.1-A.4 for examples of particle spectra and images in the other defined categories). The spectra of alumino-silicates should not inherently show high abundances of carbon; however, due to the small size of respirable dust, the carbon peak in the “alumino-silicate” spectrum in Figure 2.2 is the second highest peak, after oxygen. The phenomenon of increasing carbon content with decreasing particle size is applicable for all defined dust categories.

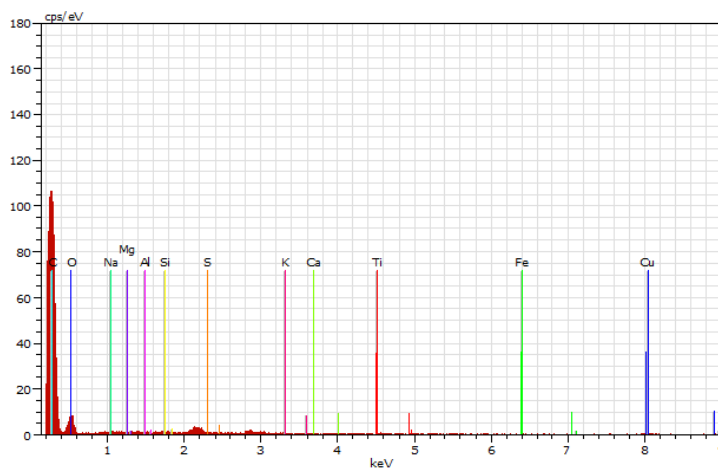


*Figure 2.1. Example spectrum of the PC filter media. The red peak on the left side of the spectrum is the peak associated with carbon, and the peak to the right of carbon is the oxygen peak. The small peaks between 2 and 3 keV are the peaks from the Au/Pd sputter coating, which should be present in all spectra when Au/Pd is used to coat the samples.*

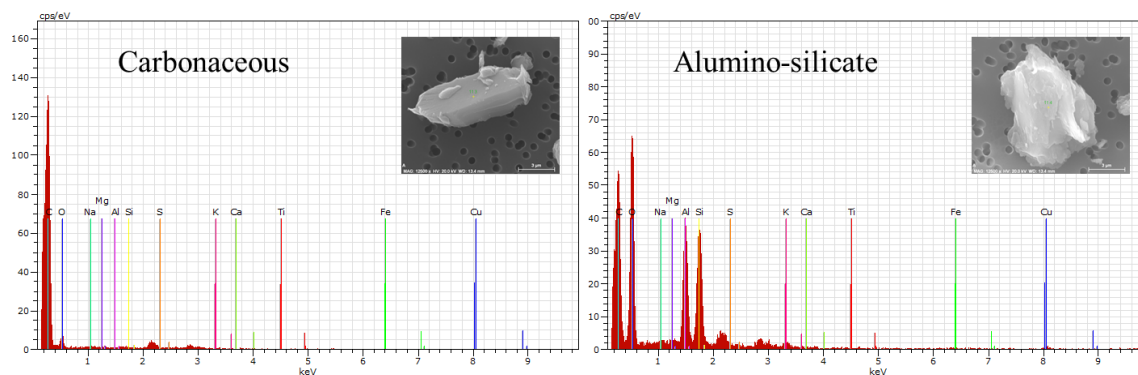


*Figure 2.2. Comparison of example spectra and images for carbonaceous (left) and alumino-silicate (right) particles at 12,500x magnification. The spectrum for the carbonaceous particle ( $L=9.87 \mu\text{m}$ ) has a relatively large carbon peak and a much smaller oxygen peak, while the spectrum for the alumino-silicate particle ( $L=11.24 \mu\text{m}$ ) has relatively large oxygen and carbon peaks, and aluminum and silicon peaks of similar height.*

To determine the particle size at which electron penetration depth may result in apparently enhanced carbon peaks, an experiment was conducted that examined quartz particles of decreasing size. To investigate, a ROM lab-generated dust sample was collected onto a PC filter. Under the SEM, the filter was scanned for quartz particles of varying sizes (i.e., long dimensions ( $L$ ) of  $0.7 \mu\text{m}$ ,  $1 \mu\text{m}$ ,  $1.5 \mu\text{m}$ ,  $2 \mu\text{m}$ ,  $2.5 \mu\text{m}$ ,  $3.5 \mu\text{m}$ ), and EDX spectra were observed for each.  $L$  is simply the longest dimension visible for the particle (see e.g., Sneed and Folk, 1958). Results showed that carbon peaks were higher for smaller particles; to be specific, particles with  $L \geq 1.5 \mu\text{m}$  had carbon peaks  $< 80 \text{ Cps/eV}$  and silicon peaks  $> 50 \text{ Cps/eV}$ , while particles with  $L < 1.5 \mu\text{m}$  had carbon peaks approximately  $80 \text{ Cps/eV}$  and silicon peaks approximately  $20 \text{ Cps/eV}$ . Thus, particles with  $L \ll 1.5 \mu\text{m}$  may have exceedingly small DE peaks; and, the rules for classifying such particles into each compositional category should make allowances for their larger carbon peak due to the probability of electron penetration and/or scatter.

The carbon content in the dust particles is particularly interesting for the “mixed carbonaceous” category. As described in Table 2.1, this category includes particles that are likely clays with some biogenic component. Considering the diagenesis of coal and surrounding sedimentary rock formations such as black shales, it is reasonable to expect that some mineral particles may indeed include organic carbon content. Another possible particle type in this category may be alumino-silicate particles that are coated with ultrafine coal dust, or alumino-silicates which are extremely platy such that the electron penetration dominates the spectrum

results. Whichever the case, spectra that are characteristic of alumino-silicates but that also have relatively large carbon peaks are classified as “mixed carbonaceous.” Although many of the other particle compositions, such as quartz or carbonate, had particles with high carbon peaks, it is likely that these peaks are due to electron penetration. With the considerably small size of respirable particles, it is unlikely that these particles are due to unliberated dusts (e.g., quartz particles ingrained in carbonaceous dust).

To determine the minimum carbon content that permits classification into the mixed carbonaceous category, experiments were conducted to gain further insights on 1) whether carbon peaks would be observed from alumino-silicate particles when the background media was not allowed to interfere with EDX analysis, and 2) if the origin of some of the mixed carbonaceous dust can be defined.

The first experiment was aimed at determining if EDX spectra from “mixed carbonaceous” particles actually exhibit high carbon peaks due to their composition (indicative of biogenic content or ultra-fine coal dust coating), or if such peaks are simply an artifact of significant electron penetration. An ROM dust sample was collected onto a PC filter, and then some of the dust particles were transferred onto copper tape and prepared for SEM analysis by the usual sputter coating routine; the copper tape ensured that any electron penetration would not result in an enhanced carbon peak, but rather in copper peaks. Particles with  $L > 5 \mu\text{m}$  whose EDX spectra exhibited relatively high aluminum and silicon peaks were specifically studied. Upon analysis of 30 such particles, four spectra were found to have carbon peaks  $> 80 \text{ Cps/eV}$ . These results indicate that “mixed carbonaceous” particles can indeed exist in coal mine dust, either from ultrafine coal dust coating the particles or as biogenic minerals.

The second experiment was conducted in attempt to determine whether “mixed carbonaceous” particles are more likely of biogenic origin or simply alumino-silicates that are coated with ultra-fine coal dust. An ROM sample was collected onto a polyvinyl chloride (PVC) filter, and the entire sample was ashed using thermogravimetric analysis (TGA). The residual matter as a result of the ashing was transferred to a PC filter and the sample was prepared for SEM analysis as described above. EDX spectra revealed the presence of alumino-silicate particles with little or no carbon peaks. These results may indicate that many of the mixed carbonaceous dusts are simply coated with fine carbonaceous material; however the appearance

of the residual particles was slightly different. A change in particle morphology could also indicate a biogenic origin (i.e., the organic carbon was ingrained in the particle), as the particles were more clustered together and less angular in shape compared to previously analyzed ROM samples. Although these experiments gave some insight as to the influence of a carbon based background, it is still unclear whether these mixed carbonaceous particles are the result of ultrafine coal, biogenic minerals, or merely the influence of the PC filter media.

### 3.1.2 Dimensions

(*L*) and intermediate (*I*) dimensions of any particle analyzed can be determined directly from the SEM images using standard “line measurement” tools included in the SEM imaging software (FEI, Hillsboro, OR). *I* is the longest dimension perpendicular to *L*, which was defined above, in the same plane (Sneed and Folk, 1958). Following direct measurement of *L* and *I* (in  $\mu\text{m}$ ), the short or third-dimension (*S*) can be estimated. Theoretically, *S* is the length dimension of a particle measured at a right angle to the plane in which *L* and *I* have been found; so *S* essentially describes particle thickness. Since different minerals have characteristic shapes, a unique ratio between *S* and *I* can usually be defined for a given mineral type. Alumino-silicate particles, for example, tend to be relatively flat with relatively small *S:I* ratios, whereas quartz particles tend to be thicker with higher *S:I* ratios. Thus, based on the compositional classification of each dust particle by EDX and its measured *I* value, its *S* value (in  $\mu\text{m}$ ) can be estimated by Equation 2.1. For the particle characterization methodology developed here, the following *S:I* ratios have been assigned to each of the six defined compositional categories of interest: “carbonaceous” = 0.6, “mixed carbonaceous” = 0.5, “alumino-silicate” = 0.4, “quartz” = 0.7, “carbonate” = 0.7 and “heavy mineral” = 0.7. The *S:I* ratio is similar to the aspect ratio generally used in the field of sedimentology (e.g., see Weber et al., 2014). These values are based on those commonly used in the field of sedimentology and extensive experience of the authors in electron microscopy analysis of mineral particulates. The “mixed carbonaceous” *S:I* ratio is an average of the “carbonaceous” and “alumino-silicate” values. Dust characterized as “other” will not be assigned *S:I* ratios, thus limiting the influence of these particles to compositional distributions.

$$S = (S:I \text{ ratio}) * I \quad (\text{Eq. 2.1})$$

### 3.1.3 Shape, Volume and Mass

A variety of shape factors can also be computed for particles, including a measure of maximum projection sphericity ( $\Psi_p$ ) and the cross-sectional ( $d_c$ ) and spherical ( $d_s$ ) diameters. The  $\Psi_p$  value can be determined from the  $L$ ,  $I$  and  $S$  dimensions using Equation 2.2, which was derived by Sneed and Folk (1958).  $\Psi_p$  is a dimensionless quantity and values range between 0 and 1; values that approach 1 are associated with particle shapes that are increasingly spherical (i.e.,  $L$ ,  $I$  and  $S$  are very similar), whereas values that approach 0 are associated with particle shapes that exhibit relatively small  $S$  dimensions as compared to  $L$  and  $I$ . The  $d_c$  and  $d_s$  values (in  $\mu\text{m}$ ) can be computed from Equations 2.3 and 2.4, respectively. The cross-sectional diameter is the only calculated value based entirely on measured properties of particle size and is only accurate if the particle is a perfect sphere. The spherical diameter is more commonly used and is considered a better approximation of the particle size in aerodynamic applications (Hinds, 1999). Further, the spherical volume ( $V$ ) can also be computed (in  $\mu\text{m}^3$ ) from Equation 2.5. By assigning approximate density values ( $\rho$ ) to each compositional category, the particle masses ( $m$ ) can additionally be estimated (in  $\mu\text{g}$ ) using Equation 2.6. Based on average densities for the primary minerals expected in each of the six defined compositional categories (i.e., see USGS, 2014), the following  $\rho$  values (in  $\text{g}/\text{cm}^3$ ) have been assigned: “carbonaceous” = 1.4, “mixed carbonaceous” = 2.0, “alumino-silicate” = 2.5, “quartz” = 2.6, “carbonate” = 2.7 and “heavy mineral” = 4.0. The “mixed carbonaceous” density is an average of the “carbonaceous” and “alumino-silicate” densities.

$$\Psi_p = \left(\frac{S^2}{L \cdot I}\right)^{1/3} \quad (\text{Eq. 2.2})$$

$$d_c = \frac{L \cdot I}{2} \quad (\text{Eq. 2.3})$$

$$d_s = \Psi_p * L \quad (\text{Eq. 2.4})$$

$$V = \frac{4}{3} * \pi * \left(\frac{d_s}{2}\right)^3 \quad (\text{Eq. 2.5})$$

$$m = V * \rho * 10^{-6} \quad (\text{Eq. 2.6})$$

In addition to the shape factors noted above, particle angularity might also be considered. Angularity is an effective measure of the sharpness of the edges of a particle and, in the context of coal mine dusts, may be important in controlling interactions between respired particles and lung tissue. Angularity can be rigorously determined by measuring the observed angles of particles on SEM images; however, particularly for small particles (i.e., with  $L \leq 5 \mu\text{m}$ ), such analysis would require significant time. Given that a stated goal of the dust characterization method developed here was to efficiently collect data, it was therefore decided that a qualitative evaluation of angularity should be employed; practically, this allows for collection of some potentially valuable information without requiring excessive analytical time. This type of classification of angularity has historically been applied to particles in the micrometer size range (Liebhard and Levy, 1991; Stachowiak, 1998). To qualitatively describe angularity, particles selected for characterization should be classified as “rounded” (*r*), “transitional” (*t*), or “angular” (*a*) by the SEM user, see Figure 2.3 (Powers, 1953).

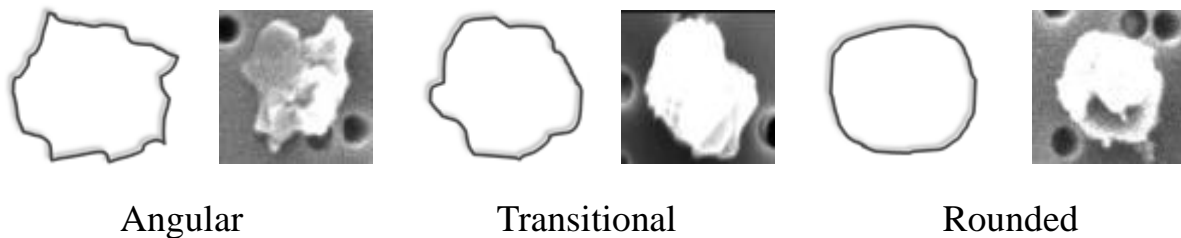


*Figure 2.3. Angularity classification categories based on the qualitative analysis of the sharpness of particle edges*

### ***3.2 General Procedures for Dust Characterization***

In order to successfully analyze samples in a methodical manner, the collection, filter preparation, and analytical process should be sound. The following steps are outlined to provide the user with a detailed protocol to efficiently and effectively characterize respirable dust samples.

### 3.2.1 Sample Collection and Filter Preparation

For collection of respirable dust samples in the field for SEM-EDX analysis, an appropriate pump deemed permissible for use in underground coal mines must be used; at present, the MSA Escort ELF pump is almost exclusively used for such applications because it has the capability to maintain near constant flow rate under a variety of environmental conditions (Gero et al., 1997). To ensure collection of only respirable dust particles, and thus rejection of particles above the respirable range, the pump should be operated with a cyclone at a flow rate between about 1.7-2.2 L/min (Khan, 2013), such that the cyclone median cut point is 4  $\mu\text{m}$  according to the NIOSH 0600 method of sampling (NIOSH, 1998). While compliance dust samples used for determining respirable mass concentration are generally collected on pre-weighed PVC filters, samples to be analyzed by SEM-EDX should be collected on PC, because they provide a suitable substrate (i.e., background media) for electron microscopy (De Bock et al., 1994; Katrinak et al., 1995; Laskin and Cowin, 2001). Filter cassettes should be unassembled two or three-piece types, such that the filters can be easily removed from the cassette for analysis.

In preparing the dust samples for SEM-EDX analysis, filter cassettes are carefully unassembled and the filters are removed with clean tweezers. On a clean surface, a 9-mm diameter trephine and a clean razorblade are used to extract the center of the filter<sup>3</sup>. This filter sub-section is then attached to an SEM pin-stub mount with double-sided tape (e.g., copper, carbon), and sputter coated with gold/palladium (Au/Pd) to create the conductive surface layer needed for electron microscopy analysis. It should be noted that carbon sputter coating cannot be used since this will interfere with composition analysis by EDX of the dust particles containing carbon, but other sputter coatings (e.g., platinum, Pt) might be considered. During development of the characterization method, it was observed that a coating thickness of about 10-20 nm (i.e., 60-second sputtering time) was optimal for preventing sample charging while allowing sufficient electron interaction with the dust particles to provide high-resolution SEM images and EDX spectra.

---

<sup>3</sup> The sub-section removed for analysis represents approximately 6% of the 37 mm filter. It is recognized that particle uniformity as a function of particle size may be variable for these types of filters, which can result in larger particles depositing toward the center (Baron, 2003); yet deposition is fairly radially symmetric (Miller et al., 2013). Center filter analysis has been shown to provide reasonably precise results for field samples using two or three-piece cassettes (Miller et al., 2013). As the main objective here is to provide relative comparisons between center filter sub-sections, some work has been completed to demonstrate that particles  $> 0.5\mu\text{m}$  are uniformly distributed by number across the sub-section (see below for details).

### 3.2.2 Particle Selection and Analysis by SEM-EDX

Following dust sample collection and filter preparation, SEM-EDX is used for particle characterization. Although equivalent equipment could be used, for the method outlined in this paper the same equipment and software, described above, was utilized. The developed method utilizes images obtained from a secondary electron (SE) detector for physical characterization of the dust particles (i.e., to measure dimensions and qualitatively evaluate particle angularity), and EDX spectra for compositional analysis.

In order to select particles for characterization without bias, a rigorous routine was developed to navigate the prepared 9-mm diameter filter sub-sections under the SEM. The routine was developed using an iterative process, whereby over 700 particles in total from the lab-generated dust samples were interrogated for elemental composition, long and intermediate dimensions and estimated shape factors (all described in detail below). With each iteration of analysis, the routine was improved until nearly all particles encountered could be quickly classified into one of the pre-determined compositional categories described above using the EDX spectra, and raw size and shape data could be efficiently gathered for later computational analysis. It is important to note that this routine was developed based on the assumption that somewhere between 50-150 particles would be analyzed per dust sample, with fewer particles limiting the statistical power of results and more particles limiting practicality due to time requirements. During preliminary verification of the dust characterization method, a simple evaluation of the effect of number of particles analyzed (i.e., statistical sample size) on resulting compositional distribution was conducted (see below). Ultimately, it was determined that analysis 100 particles per sample provided enough information about the sample while maintaining reasonable analytical time requirements (i.e., about 75-90 minutes per sample). A detailed description of the particle selection and analysis routine follows.

First, the SEM should be focused at a magnification of 10,000x, which will allow for analysis of particles within the desired size range (i.e., about 0.5-8 $\mu$ m); a somewhat higher magnification could be used if the particle size distribution is relatively small (i.e., there are few large particles), but significantly lower magnification will prohibit adequate resolution for analysis of finer particles. With the line measurement tool, two horizontal lines are then drawn 2  $\mu$ m apart and spanning the entire width of the screen, such that the space between the lines is centered on

the screen (Figure 2.4). The SEM is then positioned such that the dust characterization will begin in the top left-hand portion of the prepared filter subsection, approximately three screen shifts from its outer edge and approximately 2.25 mm from the top (i.e., one quarter of the diameter) (Figure 2.5). Three screen shifts from the edge of the filter prevents analysis of any particles disturbed during the filter sub-sectioning process. Also, the placement of the SEM stub inside the instrument determines the orientation of the “top” of the stub, based on the upper border of the screen.

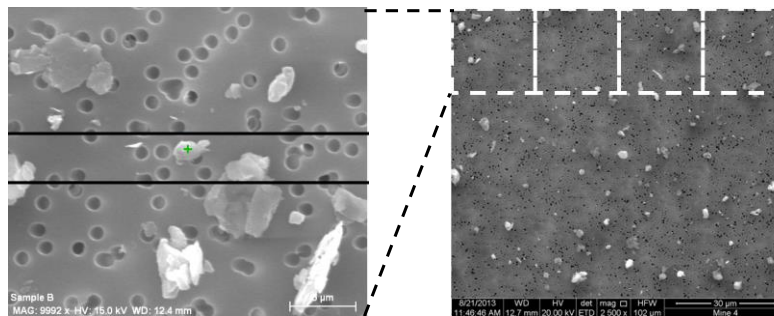


Figure 2.4. Example of particle selection and screen shifting via the joystick. The image on the left illustrates analysis of particles intersecting between the two lines in the center of the screen at 10,000x magnification. The image on the right, at 2,500x magnification, shows four screens, each outlined in a white dotted line, where analysis (at 10,000x magnification) will take place consecutively.

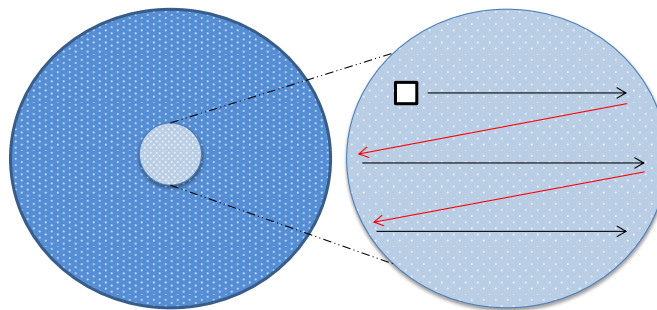


Figure 2.5. Illustration of 9 mm diameter filter sub-section and navigation routing for SEM-EDX analysis. The image on the left is the whole 37 mm diameter filter and the image on the right depicts the sub-section removed for analysis. The box in the top, left corner of the filter sub-section illustrates the first frame (i.e. field of view) in which particles should be selected for characterization; the black arrows in the filter sub-section define the directions for successive screen shifts between characterization frames. When one horizontal line of analysis is complete (black arrow directions), the red arrows define shifting back to the left side of the filter to continue analysis.

Once the instrument is focused and initially positioned, selection and analysis of dust particles can begin. Moving from left to right on the screen, each particle with  $L > 0.5 \mu\text{m}$  that intersects the space between the two horizontal lines and falls completely within the field of view should be selected for analysis; if no particles in the field of view fit these criteria, the next field to the right can be examined, and so on (see below.) Particles with  $L < 0.5 \mu\text{m}$  are too small to produce quality spectra results – if analysis of smaller particles is critical, transmission electron microscopy (TEM) would be better suited for this application (Rice et al., 2013). In an effort to analyze more of the filter area, in regards to high dust density samples, a maximum of 10 particles (i.e., the first 10 that meet the above criteria moving from left to right) per field of view should be analyzed. This would allow a minimum of 10 fields of view in order to characterize 100 particles.

At the approximate center of each particle selected for analysis, the “spot” (or analogous) analysis function on the SEM software can be used with in conjunction with the EDX software to generate elemental spectra. Based on the rules outlined in Table 2.1, the particle can be classified into one of the seven compositional categories. Additionally, the  $L$  and  $I$  dimensions of each selected particle should be measured using the built-in line measurement tools in the SEM software. Finally, angularity should qualitatively classified into one of the three categories described above (Figure 2.3). After recording raw data (i.e.,  $L$ ,  $I$ , angularity, and composition), the user can proceed to the next particle selected for analysis. Once all eligible particles (i.e., based on the criteria above) in the current field of view have been analyzed, the user should proceed to the next field of view (i.e., moving to right per Figures 2.4 and 2.5) for selection and analysis of more particles.

The above steps should be followed until analysis reaches the right-hand side of the filter subsection, approximately three screen shifts from its edge, or until 100 particles have been analyzed, whichever comes first. If 100 particles have not yet been analyzed, the user should navigate back to the left side of the filter subsection (see top red arrow in Figure 2.5), and reposition the SEM such that the field of view is approximately three screen shifts from the outer edge of the filter subsection and approximately 4.5 mm from the top (i.e., half of the diameter). From this position, particles should again be selected for analysis by scanning from left to right within the current field of view and adhering to the criteria outlined above; then, analysis should

proceed to the next field of view. If the user again reaches the right side of the filter subsection before 100 particles are analyzed, the SEM can be repositioned back to the left – this time approximately three screen shifts from the left edge of the filter subsection and approximately 6.75 mm from the top (i.e., three-fourths of the diameter). Particle selection and analysis should proceed as before.

### ***3.3 Automated Analysis Program***

To automate analysis of the raw data collected from SEM images and EDX spectra, a spreadsheet program was also developed using Microsoft Excel 2010 (Microsoft, Redmond, WA). For each dust particle, the user inputs the compositional classification (i.e., per Table 2.1), measured dimensions ( $L$  and  $I$ ), and qualitative angularity classification (i.e.,  $r$ ,  $t$  or  $a$ ), and the program then computes the following characteristic quantities based on the assigned  $S:I$  ratios and  $\rho$  values for each compositional category and Equations 2.1-2.6: short dimension ( $S$ ), maximum projection sphericity ( $\Psi_p$ ), cross-sectional diameter ( $d_c$ ), spherical diameter ( $d_s$ ), volume ( $V$ ), and mass ( $m$ ). Subsequently, distributions of composition, size (i.e.,  $d_s$ ) and angularity (either by particle number or mass) can be automatically generated for each dust sample. While composition and angularity classifications are inherently categorical (i.e., each particle has been placed into a specific composition or angularity category by the SEM-EDX user), particle size is continuous (i.e., the computed spherical diameter is numeric quantity.) Thus, to generate distributions of quantities based on particle dimensions, a number of size categories (or classes) was defined; for this, a logarithmic base 2 scale was used, which is a common approach used to classify particles based on work done by Wentworth (1922). Here, the automated program considers a total of nine size classes from  $> 0.125 \mu\text{m}$  to  $> 16 \mu\text{m}$ .

The spreadsheet program additionally includes input cells for general sample information (e.g., sample name or number, description of collection location or conditions, total filter area and filter sub-section area, total number of particles characterized, total linear length of filter analyzed), and provides basic output based on that information (e.g., percent of total filter analyzed, approximated particle density on the sub-section by mass or number). Appendix A, provides example screenshots of the program spreadsheets for data entry and output. A number of graphical representations of the data results are also generated for each sample.

#### **4. Preliminary Verification of Developed Characterization Method**

In order to provide some preliminary verification of the characterization method developed for coal mine dust by SEM-EDX, three field samples were collected and analyzed according to the guidelines outlined above. In particular, the objectives were to: 1) verify that analysis of 50-150 particles per sample is sufficient to describe the compositional, size, and shape distributions on the filter sub-sections; and 2) verify that the six defined compositional categories using the lab-generated dust samples from ROM material, and rules for classification of particles into each category, do indeed allow characterization of the majority of particles from real field samples (i.e., do most particles fit into one of these categories, or are many particles being classified as “other”?) It should be noted that insights gained from a previous study<sup>4</sup> already provided verification that particle deposition (by number) on the filter sub-sections is generally uniform.

##### ***4.1 Materials***

The dust samples used for method verification were collected from the same underground coal mine where the ROM sample used for method development originated. An Escort ELF pump with a Dorr-Oliver cyclone was used to collect the samples onto 37 mm PC filters, and each sample was collected over a period of about 120 minutes. The first sample, “Roof Bolter”, was collected from a location adjacent to a roof bolting machine, and thus was expected to contain relatively high proportions of alumino-silicate and possibly quartz particles (vs. other compositions) due to the drilling activity of the machine into roof material. The second sample, “Belt Drive”, was collected from a location just above a belt drive, where coal and rock were being transported below on a conveyor belt. The “Belt Drive” sample was anticipated to include greater proportions of carbonaceous particles, and some carbonate particles were also expected

---

<sup>4</sup> The question of particle distribution has already been addressed in Sellaro and Sarver, 2013. In summary, particle quantification was completed on four different areas (at 2,500x magnification) of filter sub-sections from 17 different field samples; this involved counting all particles with  $L$  dimensions  $> 0.5 \mu\text{m}$  in each of the four areas, which were each located in a different quadrant of the filter sub-section. Particle counts were determined to be similar (i.e., based on a 95% confidence interval) between each of the four areas for all but two samples. These specific filters had one quantification area with many agglomerated particles, as opposed to few, separate particles, viewed on the other three quantification areas. The agglomeration in these samples is thought to be due to humidity throughout the intake airway of the mine, where both were collected.

due to heavy rock dusting in the belt entries. (Rock dusting is a practice used to limit propagation of coal dust explosions, and requires walls and floors to be covered with fine inert material such as  $\text{CaCO}_3$ .) The third sample, “Intake”, was collected from a location near the working section of the mine in intake air (i.e., fresh air being delivered to the mine by its ventilation system). The “Intake” sample was expected to have relatively similar proportions of carbonaceous and alumino-silicate particles, with some carbonate due to rock dusting in the area. Estimated particle densities on the “Roof Bolter”, “Belt Drive”, and “Intake” filter sub-sections were 16,292 particles/ $\text{mm}^2$ , 12,639 particles/ $\text{mm}^2$ , and 1,850 particles/ $\text{mm}^2$ , respectively. These densities were extrapolated from the average number of particles counted in four different areas on each sub-section; each area was  $10,404 \mu\text{m}^2$  and located in a different quadrant of the sub-section areas. Figure 2.6 displays SEM images for each sample.

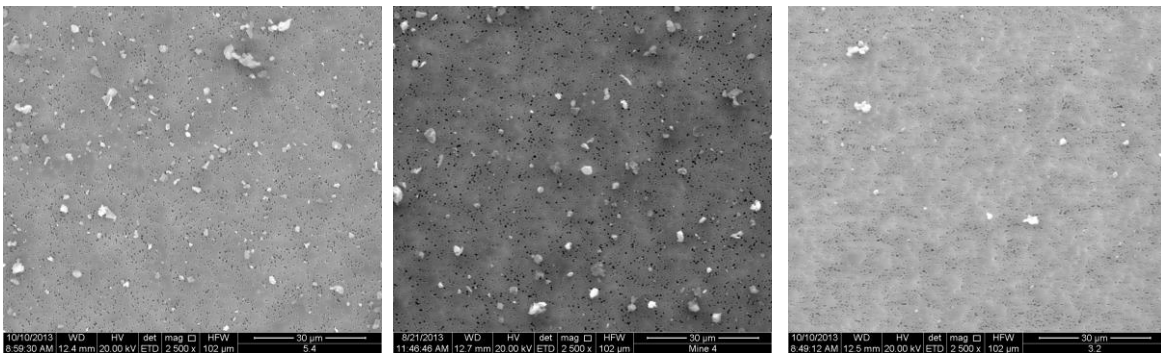


*Figure 2.6. SEM images at 2,500x magnification for the filter sub-sections from each verification sample showing relative particle densities. The far left image represents the “Roof Bolter”, followed by the “Belt Drive” image, and finally the “Intake” image on the right.*

#### **4.2 Results and Discussion**

To evaluate the effects of number of particles analyzed ( $n$ ) on dust sample characterization results, compositional distributions by particle number and mass were compared for a range of  $n$  values (Table 2.2). For the “Roof Bolter” and “Belt Drive” samples, 200 particles in total were analyzed, and the resultant compositional distributions were compared for the first 25, 50, 100, 150, and 200 particles (i.e.,  $n = 25, 50, 100, 150$  or  $200$ ); for the “Intake” sample, only 100 particles were analyzed in total, so  $n$  values of 25, 50, and 100 were compared. Somewhat surprisingly, when comparing compositional distribution of particles by number, all samples

showed relatively similar results across all  $n$  values – meaning that even when  $n$  was increased by 4-8x, little change was observed in the relative number of particles being classified into each compositional category. When comparing compositional distribution by mass, however, only the “Belt Drive” sample produced similar results across all  $n$  values. For the other two samples, as  $n$  increased, the distributions changed significantly. For example, in the “Roof Bolter” sample, the first 100 particles analyzed showed very little carbonaceous material on a mass basis, but first 150 particles analyzed showed that over a quarter of the mass was due to carbonaceous particles. This particular discrepancy was traced to a single very large coal particle ( $d_s > 5 \mu\text{m}$ ) that was selected for analysis based on the developed dust characterization method, and it underscores a key challenge that aerosol scientists and industrial hygienists often face when studying or reporting on particulates. Indeed, due to limitations in analytical equipment and the efficiency of bulk analyses, environmental monitoring and regulation of airborne particulates is often based on mass rather than number concentrations.

In consideration of the results presented in Table 2.2, and the typical times required for SEM-EDX analysis for different  $n$  values, it was determined that analysis of 100 total particles per sample should be both sufficient (at least for describing sample distributions by particle numbers) and practical for the developed dust characterization method. Further work may be needed, however, to determine if or how few, relatively large particles in a sample are contributing to its characteristics on a mass basis. If required, simple additional steps could be incorporated into the developed characterization method to quickly gather more data in this regard (e.g., visually scanning the filter sub-section at a relatively lower magnification to assess density of large particles, or elemental mapping at a relatively lower magnification to assess compositional differences in larger particles.)

Also from Table 2.2, it appears that the six pre-determined compositional categories, and rules outlined in Table 2.1 for particle classification, can account for most respirable particles in expected in dust samples from underground coal mines. Indeed, of the 500 total particles analyzed across all three samples, none required classification into the “other” category. It should of course be noted that dust composition could vary with varying coal and rock geologies, and mining and operational practices – and thus between mines. So, further verification of the

developed method for dust characterization should certainly be conducted using samples collected from multiple mines/regions of interest.

*Table 2.2. Distribution of particle composition by number (and mass) for the method verification samples. All values are rounded to the nearest whole number*

| <b>Roof Bolter</b> | <b>25 Particles</b> | <b>50 Particles</b> | <b>100 Particles</b> | <b>150 Particles</b> | <b>200 Particles</b> |
|--------------------|---------------------|---------------------|----------------------|----------------------|----------------------|
| Carbonaceous       | 12% (1%)            | 12% (2%)            | 11% (3%)             | 11% (27%)            | 12% (21%)            |
| Mixed Carbonaceous | 36% (31%)           | 28% (25%)           | 32% (19%)            | 33% (26%)            | 35% (23%)            |
| Alumino-Silicate   | 48% (68%)           | 50% (64%)           | 49% (67%)            | 47% (39%)            | 45% (41%)            |
| Quartz             | 4% (0%)             | 8% (7%)             | 6% (10%)             | 6% (6%)              | 7% (8%)              |
| Carbonate          | 0% (0%)             | 0% (0%)             | 0% (0%)              | 0% (0%)              | 0% (0%)              |
| Heavy Mineral      | 0% (0%)             | 2% (2%)             | 2% (1%)              | 3% (2%)              | 3% (7%)              |
| Other              | 0% (0%)             | 0% (0%)             | 0% (0%)              | 0% (0%)              | 0% (0%)              |
| <b>Belt Drive</b>  | <b>25 Particles</b> | <b>50 Particles</b> | <b>100 Particles</b> | <b>150 Particles</b> | <b>200 Particles</b> |
| Carbonaceous       | 20% (27%)           | 24% (40%)           | 29% (37%)            | 26% (36%)            | 24% (27%)            |
| Mixed Carbonaceous | 20% (3%)            | 24% (7%)            | 21% (5%)             | 21% (5%)             | 25% (5%)             |
| Alumino-Silicate   | 32% (62%)           | 30% (40%)           | 30% (46%)            | 33% (48%)            | 30% (47%)            |
| Quartz             | 4% (0%)             | 2% (0%)             | 4% (1%)              | 3% (1%)              | 5% (2%)              |
| Carbonate          | 8% (1%)             | 12% (9%)            | 12% (10%)            | 12% (9%)             | 14% (18%)            |
| Heavy Mineral      | 16% (7%)            | 8% (4%)             | 4% (1%)              | 5% (1%)              | 4% (1%)              |
| Other              | 0% (0%)             | 0% (0%)             | 0% (0%)              | 0% (0%)              | 0% (0%)              |
| <b>Intake</b>      | <b>25 Particles</b> | <b>50 Particles</b> | <b>75 Particles</b>  | <b>100 Particles</b> |                      |
| Carbonaceous       | 32% (56%)           | 40% (50%)           | 44% (44%)            | 45% (48%)            |                      |
| Mixed Carbonaceous | 20% (2%)            | 16% (4%)            | 17% (33%)            | 16% (30%)            |                      |
| Alumino-Silicate   | 40% (22%)           | 36% (25%)           | 31% (12%)            | 32% (14%)            |                      |
| Quartz             | 4% (1%)             | 2% (1%)             | 1% (0%)              | 2% (0%)              |                      |
| Carbonate          | 4% (19%)            | 2% (16%)            | 1% (7%)              | 1% (6%)              |                      |
| Heavy Mineral      | 0% (0%)             | 4% (4%)             | 5% (3%)              | 4% (3%)              |                      |
| Other              | 0% (0%)             | 0% (0%)             | 0% (0%)              | 0% (0%)              |                      |

To demonstrate the robustness of the developed dust characterization method, size distributions, again by particle number and mass, for the three verification samples were also generated by the automated spreadsheet program (Figs. 2.7-2.12). The influence that large particles can have on mass-based data is reiterated by examining the “Roof Bolter” results (Figures 2.7-2.8), which indicate that 1% of the total particles fell into the 4-8  $\mu\text{m}$  size class, but these make up 19% of the total mass. Figure 2.13 shows the relative angularity of particles in the “Intake” sample, with results broken down between compositional categories.

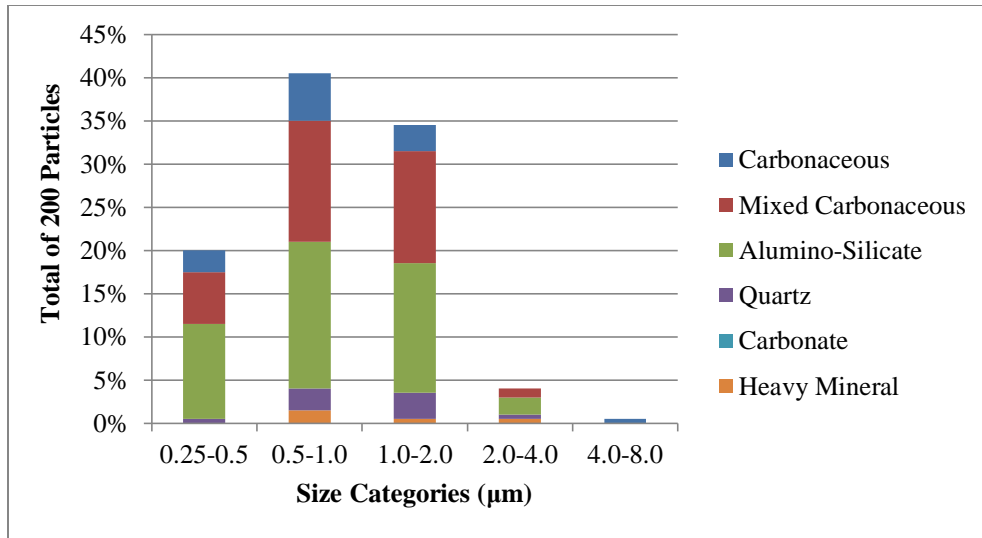


Figure 2.7. Particle size distribution by number for the Roof Bolter sample; the relative number of particles in each compositional category is shown within each bar.

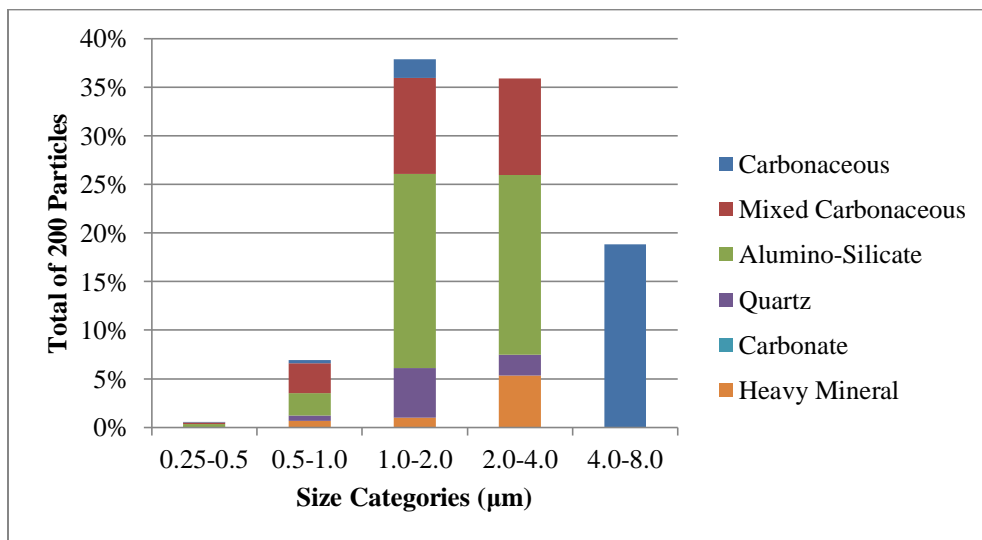


Figure 2.8. Particle size distribution by mass for the Roof Bolter sample; the relative mass of particles in each compositional category is shown within each bar.

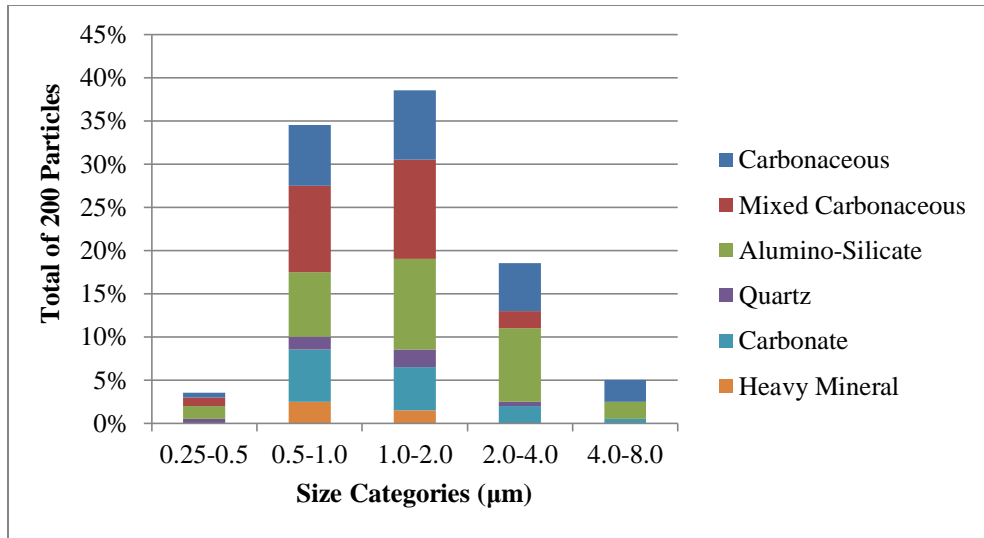


Figure 2.9. Particle size distribution by number for the Belt Drive sample; the relative number of particles in each compositional category is shown within each bar.

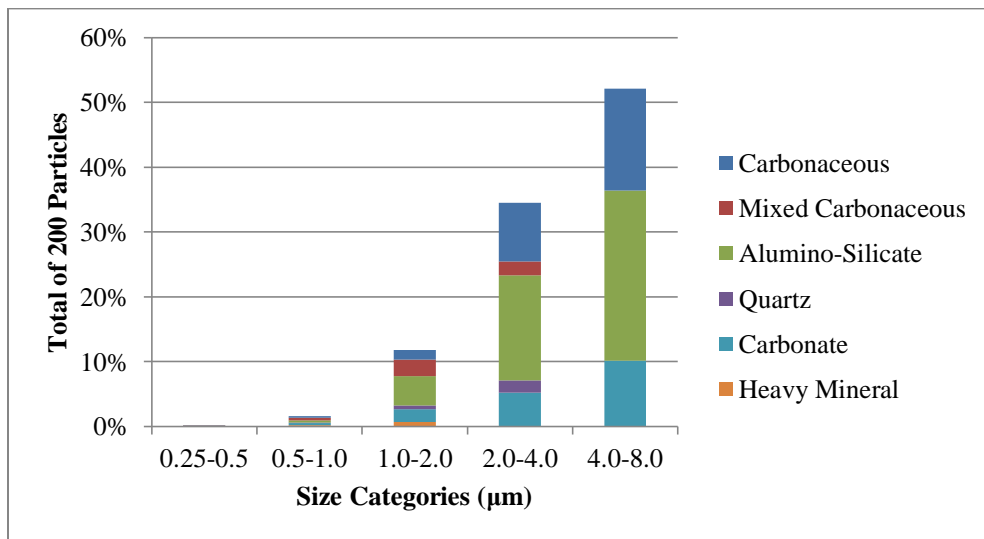


Figure 2.10. Particle size distribution by mass for the Belt Drive sample; the relative mass of particles in each compositional category is shown within each bar.

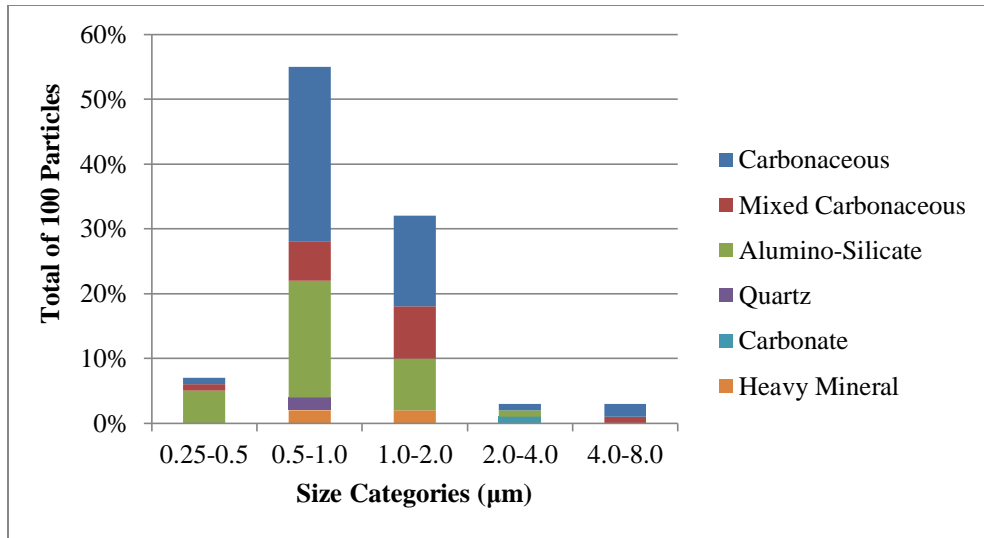


Figure 2.11. Particle size distribution by number for the Intake sample; the relative number of particles in each compositional category is shown within each bar.

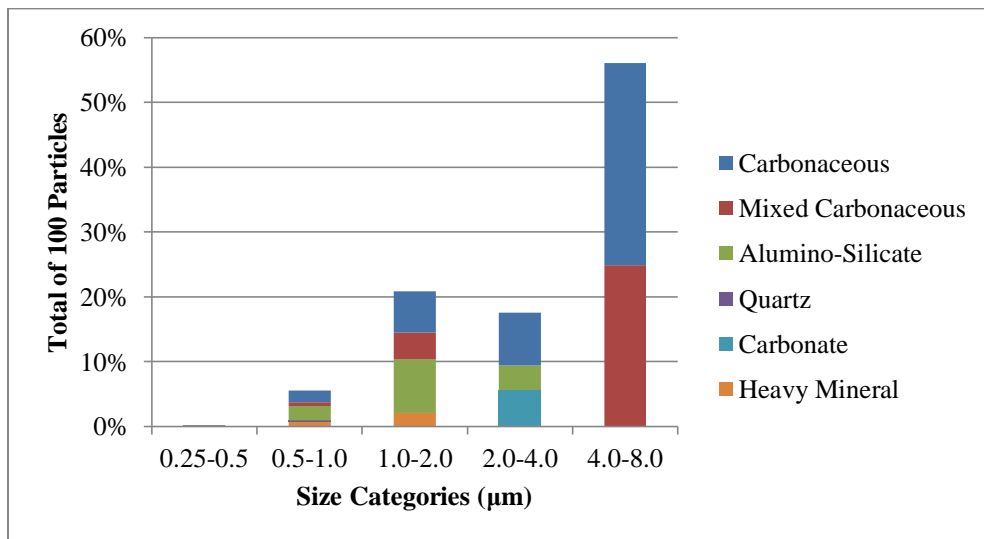


Figure 2.12. Particle size distribution by mass for the Intake sample; the relative mass of particles in each compositional category is shown within each bar.

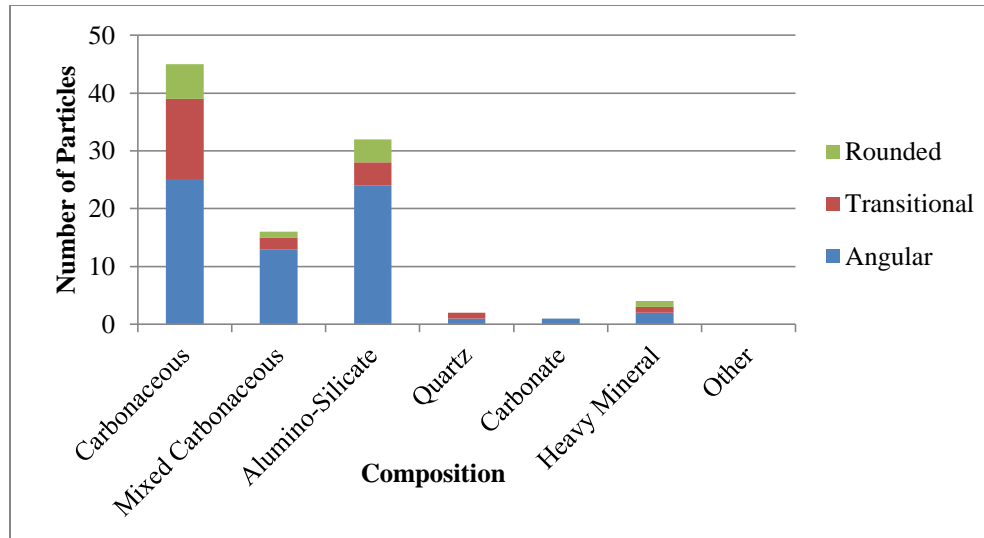


Figure 2.13. Particle compositional distribution by number for the Intake sample; the relative number of particles classified as having angular, transitional or rounded shapes is shown within each bar.

## 5. Conclusions

SEM-EDX is a powerful tool, which can be used for particle-level analysis of dust samples. This paper describes a standard methodology developed for the purpose of achieving more comprehensive characterization of respirable dusts in underground coal mines. Due to the large amounts of data that can be generated by this method, a relatively simple spreadsheet program is recommended for automating computational analyses to compare particles within and between dust samples.

Future work should be geared toward further understanding particle uniformity, by both number and size of particles, across the entire filter area and uniformity by particle size across the filter sub-section. In cases of non-uniformity, such as agglomerated dust, characterization of > 100 particles may be necessary. The method is also user specific, and the steps outlined above are at the interpretation of the user, such as in cases of exceptionally high dust density samples and increased numbers of large dust particles. Although the method outlined in this paper was shown to classify particles properly from one specific mine, to accommodate a mine of different mineralogy, the particle dust categories should be altered prior to particle classification. The time required for this type of comprehensive analysis can be a major drawback; however the use of a standard methodology may increase analytical efficiency as well as consistency.

## 6. References

- Attfield, M., Hale, J., et al. (2011). Current Intelligence Bulletin 64: Coal Mine Dust Exposures and Associated Health Outcomes – A Review of Information Published Since 1995. *DHHS (NIOSH)*, Publication No. 2011-172.
- Baron, P. (2003). Factors Affecting Aerosol Sampling, NIOSH Manual of Analytical Methods. *NIOSH/DART, O*, 184-207.
- Bruker (2014). Bruker Corporation, Ewing, NJ: Bruker Corp.
- Centers for Disease Control (CDC) (2006). Advanced Cases of Coal Workers' Pneumoconiosis- Two Counties, Virginia. *MMWR*, 55(33).
- Coal Workers' Health Surveillance Program (CWHSP) Data Query System (2014). Occupational Respiratory Disease Surveillance, Available at: <http://webappa.cdc.gov/ords/cwhsp-database.html>.
- De Bock, L., Van Malderen, H., Van Grieken, R. (1994). Individual Aerosol Particle Composition Variations in Air Masses Crossing the North Sea. *Environmental Science and Technology*, 28, 1513-1520.
- Federal Register (2014). Lowering Miner's Exposure to Respirable Coal Mine Dust, Including Continuous Personal Dust Monitors, 79 *Fed. Reg.* 24813.
- FEI (2014). FEI Company, Hillsboro, OR: FEI Corp.
- Gero, A., Parobeck, P., Suppers, K., et al. (1997). Effect of Altitude, Sampling Port Inlet Loading, and Temperature on the Volumetric Flow Rate of the MSA Escort Elf Constant-Flow-Rate Pump. *Applied Occupational Environmental Hygiene*, 12(12), 941-946.
- Hinds, W. (1999). *Aerosol Technology: Properties, Behavior, and Measurement of Airborne Particles*, 2<sup>nd</sup> Edition, New York, NY, Wiley-Interscience Publications.
- Katrinak, K., Anderson, J., Buseck, P. (1995). Individual Particle Types in the Aerosol of Phoenix, Arizona. *Environmental Science and Technology*, 29, 321-329.
- Khan, A. (2013). Characterizing the Variability in Respirable Dust Exposure using Johnson Transformtaion and Re-examining 2010 Proposed Changes to the U.S. Underground Coal Mine Dust Standard. University of Kentucky, Theses and Dissertations-Mining Engineering, Paper 5.

- Laney, A., Attfield, M. (2014). Examination of Potential Sources of Bias in the US Coal Workers' Health Surveillance Program. *American Journal of Public Health*, 104(1), 165-170.
- Laney, A., Wolfe, A., Petsonk, E., Halldin, C. (2012). Pneumoconiosis and Advanced Occupational Lung Disease among Surface Coal Miners – 16 States, 2012-2011. *MMWR*, 61(23), 431-434.
- Laskin, A., Cowin, J. (2001). Automated Single-Particle SEM/EDX Analysis of Submicron Particles down to 0.1  $\mu\text{m}$ . *Analytical Chemistry*, 73, 1023-1029.
- Liebhard, M., Levy, A. (1991). The effect of erodent particle characteristics on the erosion of metals. *Wear*, 151(2), 381–390.
- Microsoft (2010). Microsoft Excel [Computer Software], Redmond, WA: Microsoft.
- Miller, A., Drake, P., Murphy, N., et al. (2013). Deposition Uniformity of Coal Dust on Filters and Its Effects on the Accuracy of FTIR Analyses for Silica. *Aerosol Science and Technology*, 47, 724-733.
- National Institute for Occupational Safety and Health (NIOSH) (1998). NIOSH Manual of Analytical Methods, 4<sup>th</sup> Edition, Particulates Not Otherwise Regulated, Respirable: Method 0600: *Issue 3*, 1-6.
- Pollock, D., Potts, J., Joy, G. (2010). Investigation into Dust Exposures and Mining Practices in Mines in the Southern Appalachian Region. *Mining Engineering*, 62(2), 44-49.
- Powers, M. (1953). A New Roundness Scale for Sedimentary Particles. *Journal of Sedimentary Petrology*, 23, 117-119.
- Rice, S., Chan, C., Brown, S., et al. (2013). Particle Size Distributions by Transmission Electron Microscopy: an Interlaboratory Comparison Case Study. *Metrologia*, 50(6), 663-678.
- Sellaro, R., Sarver, E. (2013). Characterization of Dust in Underground Coal Mines and Implications for Occupational Health. Society of Mining Engineers (SME) Annual Meeting, Feb. 23-26, Salt Lake City, UT, Preprint 14-058.
- Sneed, E., Folk, R. (1958). Pebbles in the Lower Colorado River, Texas, a study in particle morphogenesis. *The Journal of Geology*, 6(2), 114-150.
- Stachowiak, G. (1998). Numerical Characterization of Wear Particles Morphology and Angularity of Particles and Surfaces. *Tribology International*, 31(1-3), 139-157.

- Suarthana, E., Laney, A. S., Storey, E., et al. (2011). Coal workers' pneumoconiosis in the United States: regional differences 40 years after implementation of the 1969 Federal Coal Mine Health and Safety Act. *Occupational Environmental Medicine*, 68, 908–913.
- USGS (2014). U.S. Geological Survey, Accessed at: [www.usgs.gov](http://www.usgs.gov)
- Weber, C., Heuser, M., Mertens, G., Stanjek, H. (2014). Determination of clay mineral aspect ratios from conductive titrations. *Clay Minerals*, 49(1), 17-26.
- Wentworth, C. (1922). A Scale of Grade and Class Terms for Clastic Sediments. *The Journal of Geology*, 30(5), 377-392.

## CHAPTER 3: CHARACTERIZATION OF RESPIRABLE COAL MINE DUST FROM AN UNDERGROUND COAL MINE IN CENTRAL APPALACHIA

### 1. Abstract

It has long been understood that extended occupational exposures to respirable mine dusts can lead to chronic lung disease. In underground coal mines, CWP and silicosis are major concerns. While many efforts have been aimed at understanding mass-based concentrations and silica contents of respirable dusts under a variety mining conditions, little research has been completed characterize dust at the individual particle-level (i.e., by composition, size, shape). This study employed scanning electron microscopy with energy dispersive x-ray (SEM-EDX) to analyze dust samples collected from an underground coal mine in Central Appalachia. The results indicated that particle characteristics can vary widely between locations, though many trends might be explained based on knowledge of mining conditions. A continuous personal dust monitor (CPDM) was also used during collection of some samples to determine respirable dust concentrations, which were compared to estimated concentrations based on the particle-level analysis.

### 2. Introduction

*Dust* is generally defined as small, solid particles with an effective diameter  $< 75 \mu\text{m}$  (ISO, 1995). In underground coal mines, dust is produced by a variety of activities (e.g., coal and rock cutting, materials handling, haulage) and from a variety of materials. While the coal itself is primarily made up of organic carbon, it is estimated that as much as 60% of coal mine dust consists of mineral matter, including clays, metal oxides and sulfides, carbonates, quartz, phosphates and heavy minerals (WHO, 1997). Mineral matter may be ingrained in the coal seam or associated with adjacent or inter-lying strata, and may also be contributed by specific activities like rock dusting. When dust is generated or made airborne, suspended particles tend to settle slowly with gravitational forces, but can remain airborne for extended periods of time depending on environmental conditions such as air velocity (Courtney et al., 1986) and particle properties such as size or density (ISO, 1995; WHO, 1999). Miners working underground are

routinely subject to occupational dust exposures, with highly variable characteristics between and even within mines.

Inhalable dust, which is the portion of suspended particulates that can be deposited into the nose or mouth during inhalation, can have a very wide size distribution; however, respirable dust is the fraction of inhalable particulates that can reach the lungs. These particles are generally < 10 µm in diameter and approximately 50% of the mass of respirable particles are 4.0 µm in diameter (ACGIH, 2005). Respirable dust is often responsible for occupational respiratory illnesses in miners. Coal workers pneumoconiosis (CWP), commonly referred to as “black lung,” is one of the most common respiratory diseases affecting coal miners, and is typically associated with chronic exposure to coal dust (Ross and Murray, 2004). Silicosis is another disease that may affect coal miners, and is caused by exposure to respirable crystalline silica, which may be present in coal mine dusts. This disease is particularly concerning because it can progress relatively quickly, causing massive fibrosis in the lungs (Laney et al., 2010). Chronic obstructive pulmonary disease (COPD) has also been associated with coal mining occupations and, like CWP and silicosis, can lead to reduced lung function and be fatal in some cases (Santo Tomas, 2011).

To combat dust-related illness in coal miners in the US, the Coal Mine Health and Safety Act of 1969 (CMHSA) implemented both a health surveillance program and a federal regulation of respirable dust exposures in underground coal mines (CMHSA, 1969). CMHSA set a permissible exposure limit on respirable dust concentrations at 2.0 mg/m<sup>3</sup>, except in cases where quartz (i.e. crystalline silica, SiO<sub>2</sub>) content is > 5% by mass – and then the limit is reduced according to the actual quartz content (30 CFR Part 70.101). In the four decades following CMHSA, remarkable overall reduction in CWP was achieved, with incidence rates across the US falling from above 11% in 1970-1974 to just 2% in 1995-1999 (CWHSP, 2014; Laney and Attfield, 2014). In addition to improving occupational health outcomes, limits on respirable dust also contributed to dramatic improvements in ventilation and mining practices. In recent years, however, some surveillance data indicates that incidence of CWP has actually begun to increase again in specific regions such as Central Appalachia, which includes the coalfields of southwestern VA, eastern KY and southern WV (Attfield and Seixas, 2007; CDC, 2006; Pollock et al., 2009; Suarathana et al., 2011). Partially in response to this unexpected and unexplained trend, a new “dust rule” was

published in April 2014 (Federal Register, 2014). The new rule reduces the permissible limit on respirable dust concentrations to  $1.5 \text{ mg/m}^3$  (enforceable on August 1, 2016), which represents a compromise between the previous limit and the  $1.0 \text{ mg/m}^3$  limit recommended by the National Institute for Occupational Safety and Health (NIOSH) (NIOSH, 2003).

The new rule has been met with substantial controversy since it was first proposed in 2004 (Federal Register, 2010; Dullea and Chajet, 2013; Gamble et al., 2001; Maher, 2014), as monitoring data suggests that many mines are already meeting the reduced statutory dust limit (Attfield et al., 2011), and causal factors for the aforementioned rise in CWP have not been conclusively determined. There are in fact numerous potential explanations for the rise, from the possibility of routine (but undetected) exposures to elevated dust concentrations, to the existence of specific dust characteristics that may contribute to the onset or progression of respiratory illnesses – and there is certainly an array of literature that could be used to support a focus on dust characteristics. For example, a correlation has been reported between CWP rates and coal rank (Page and Organiscak, 2002), which is a quality associated with coal properties including mineral content (Landen et al., 2011). Particle shapes and sizes may additionally have an effect on the toxicity of coal mine dusts since particle angularity (i.e., sharpness of particles edges) can influence pathogenesis. Indeed, particles with increased surface roughness and those considered less spherical may have a higher probability of infiltrating the deepest tissues of the lungs (Hassan and Lau, 2009). Increased lung deposition is also evident for particles approximately 1-2  $\mu\text{m}$  in aerodynamic diameter, with larger particles often being deposited before reaching the deep lung tissues and smaller particles not being deposited efficiently (i.e., being exhaled) (EPA, 1999; WHO, 1999). Moreover, there have been repeated suggestions that increased silica exposures may be at least partly responsible for the CWP rise noted in Central Appalachia (Attfield et al., 2011; CDC, 2012), where young miners appear to be particularly affected (Laney et al., 2012). In this region, operators are increasingly mining thinner seams of coal (i.e., “low seam” or “thin seam” coal), which requires cutting more roof and floor rock along with the coal (Suarthana et al., 2011).

While dust samples collected for demonstrating compliance with the federal regulations are routinely evaluated to determine mass-based values for total respirable dust concentration and silica content, other potentially important dust characteristics such the mineral constituency, size

and shape, of particles are rarely investigated. These characteristics may indeed be key in understanding occupational health risks and outcomes of mine workers. The purposes of this study were to 1) demonstrate the usefulness of scanning electron microscopy with energy dispersive x-ray (SEM-EDX) to perform comprehensive, particle-level analysis of coal mine dusts, and 2) compare dust characteristics associated with various locations or occupations in a “low seam” coal mine in Central Appalachia.

### **3. Materials and Methods**

A total of 21 respirable dust samples, including twelve area samples and nine personal samples, were obtained from an underground coal mine in Central Appalachia (Table 3.1). The area sample locations represented common working areas throughout the mine or specific areas where dust may be generated. The personal sample locations for machine operators were chosen as potentially high-exposure samples, and the tramming samples (i.e., taken on a moving mantrip) were chosen based on anecdotal observations by mine personnel that mantrips often tend to kick-up dust. The study mine is considered “low-seam” based on the relatively small thickness of the coal seam and the height of the entries. The average total material extraction height of the mine is 40 inches, with an average coal seam thickness of 24 inches.

Table 3.1. Dust sample descriptions separated by area or personal sample

| Area Samples      |   |                  | Personal Samples |  |                  |
|-------------------|---|------------------|------------------|--|------------------|
| Sample            | Location  | Sample Time (hr) | Sample           | Location   | Sample Time (hr) |
| <b>Data Set A</b> |   |                  |                  |  |                  |
| A1                | Intake airway, 2 km from the section                              | 2.00             | A9               | Tram, through the intake airway to the working section from the outside      | 1.00             |
| A2                | Intake airway, 1 km from the section                              | 2.00             | A10              | Bolter, roof bolter operator   | 2.00             |
| A3                | Intake airway, 30 m from the section                              | 2.00             | A11              | Miner, continuous miner operator   | 2.00             |
| A4                | Belt, 0.5 m above the conveyor belt, 1.5 m from a belt drive      | 2.00             | A12              | Tram, through the intake airway from the working section to the outside      | 0.83             |
| A5                | Duplicate of sample A4  | 2.00             | -                | -  | -                |
| A6                | Feeder, 15 m downwind of the feeder                               | 2.00             | -                | -  | -                |
| A7                | Duplicate of sample A6  | 2.00             | -                | -  | -                |
| A8                | Return airway, 15 m from the section                              | 1.25             | -                | -  | -                |
| <b>Data Set B</b> |   |                  |                  |  |                  |
| B1                | Belt, 0.5 m above a conveyor belt, 1.5 m from a belt drive        | 1.50             | B5               | Tram, through the intake airway to the working section from the outside      | 0.75             |
| B2                | Belt, 0.5 m above a conveyor belt, 1.5 m from a second belt drive | 1.50             | B6               | Bolter, roof bolter operator 1   | 1.50             |
| B3                | Feeder, 15 m downwind of the feeder                               | 1.50             | B7               | Bolter, roof bolter operator 2   | 3.00             |
| B4                | Return airway, 15 m from the section                              | 1.50             | B8               | Miner, continuous miner operator   | 1.00             |
| -                 | -   | -                | B9               | Daily activity, tram to/from the working section and work within the section | 4.83             |

The dust sampling and characterization methodology used here was previously developed and described in detail elsewhere (Chapter 2), but a brief summary follows. Samples were collected on new polycarbonate (PC) filters (37 mm diameter) using a personal dust sampling device, consisting of an Escort ELF pump with a 10 mm Dorr-Oliver cyclone. Personal samples were collected with the inlet of the cyclone attached to an individual's lapel, and area samples were collected by placing the sampling device at a likely exposure point (i.e., about 5 ft from the floor and within the main aircourse) in the fixed locations described in Table 3.1. The filters were loaded in a clean environment into new cassettes prior to entering the mine, and transported

carefully upon the completion of sampling. The pumps for Data Set A and B were operated at a rate of 2.0 and 2.5 LPM, respectively, and all samples were collected continuously for at least 45 minutes. Operating the pump at a higher flow rate decreased the cut size of the cyclone, such that the 50% cut point should be slightly  $< 4 \mu\text{m}$  for Data Set B. Although this is not consistent with the MSHA recommended sampling flow rate, the reduced cut size should only affect collection of relatively large dust particles on the filter. The influence of large particles on dust samples is discussed below.

An FEI Quanta 600 FEG environmental SEM (FEI, Hillsboro, OR) equipped with a Bruker Quantax 400 EDX spectroscope (Bruker, Ewing, NJ) was used to analyze individual dust particles on each sample filter. To prepare the filters, clean tweezers were used to remove them from the sampling cassettes and then a circular sub-section (9 mm diameter) was cut out of the center of each filter using a stainless steel trephine. Each filter sub-section was mounted to an aluminum stub using double-sided copper tape, and the stubs were sputter coated (Au/Pd) to render the surface of the sample electrically conductive.

For all samples except A2, a total of 100 particles were characterized at 10,000x magnification; see Chapter 2 for particle selection routine and detailed description of SEM-EDX analysis. For sample A2, only 74 particles were characterized due to the very low density of dust collected on the filter. Each particle was classified based on its EDX spectra into one of seven compositional categories: “carbonaceous”, “mixed-carbonaceous”, “alumino-silicate”, “quartz”, “carbonate”, “heavy mineral”, or “other”. Examples of typical minerals associated with each category are displayed in Table 3.2, along with the dominant elements for which EDX spectra peaks are observed. Additionally, the SEM images were used to make measurements of the long ( $L$ ) and intermediate ( $I$ ) particle dimensions, as well as qualitatively assess particle angularity. The  $L$  dimension is the longest dimension in the visible plane of the particle, and  $I$  is the longest dimension perpendicular to  $L$  in the same plane (Sneed and Folk, 1958). For a particle to be selected for characterization, its  $L$  value had to be  $> 0.5 \mu\text{m}$  to ensure adequate resolution for the SEM-EDX analysis at the specified magnification, which optimizes analytical capabilities and time requirements (i.e., a large number of particles can be characterized relatively quickly; see Chapter 2). After measuring  $L$  and  $I$ , the short dimension ( $S$ ), or thickness of the particle, was also estimated based on shape characteristics commonly associated with particles in each

compositional category (e.g., see Weber et al., 2014); the *S:I* ratios assumed here are shown in Table 3.2. The angularity was assessed visually based on the sharpness of the edges of each particle, which was classified as either “rounded”, “transitional” or “angular” (Liebhard and Levy, 1991; Stachowiak, 1998).

From the particle dimensions, spherical diameter ( $d_s$ ) could also be calculated by Equations 3.1 (in  $\mu\text{m}$ ), where the first term represents the maximum projection sphericity of a particle. Further, by assuming an approximate specific gravity (SG) value for each compositional category (Table 3.2), the volume (in  $\mu\text{m}^3$ ) and mass (in  $\mu\text{g}$ ) of each particle could also be estimated (Equations 3.2-3.3). Thus, particle distributions by mass and number could be evaluated for each sample. The results presented here are shown by particle number to limit the number of assumptions required, although estimated particle masses are used to compare respirable dust concentrations (i.e., reported as  $\text{mg}/\text{m}^3$ ) based on the SEM-EDX data to those derived from CPDM measurements.

$$d_s = \left( \frac{S^2}{L \cdot I} \right)^{1/3} * L \quad (\text{Eq. 3.1})$$

$$V = \frac{4}{3} * \pi * \left( \frac{d_s}{2} \right)^3 \quad (\text{Eq. 3.2})$$

$$m = V * \rho * 10^{-6} \quad (\text{Eq. 3.3})$$

*Table 3.2. Common minerals and mineral properties represented in each compositional category*

| <b>Composition Category</b> | <b>Example Mineralogy</b>           | <b>Dominant Elements</b>  | <b><i>S:I</i> Ratio</b> | <b>Specific Gravity</b> |
|-----------------------------|-------------------------------------|---------------------------|-------------------------|-------------------------|
| Carbonaceous                | Coal                                | Carbon                    | 0.6                     | 1.4                     |
| Mixed Carbonaceous          | Biogenic/Organic Carbonaceous Clays | Carbon, Aluminum, Silicon | 0.4-0.6                 | 1.4-2.5                 |
| Alumino-silicate            | Clays, Feldspars                    | Aluminum, Silicon         | 0.4                     | 2.5                     |
| Quartz                      | Crystalline Silica                  | Silicon                   | 0.7                     | 2.6                     |
| Carbonate                   | Rock Dust, Calcite, Dolomite        | Calcium/Magnesium, Carbon | 0.7                     | 2.7                     |
| Heavy Mineral               | Pyrite, Titanium Oxides             | Titanium/Iron/Aluminum    | 0.7                     | 4.0                     |
| Other                       | DPM, etc.                           | -                         | -                       | -                       |

During collection of seven of the samples in Data Set A, a CPDM was used simultaneously to record respirable dust concentrations (i.e., as 30-minute running averages), from which the average concentration during sample collection could be approximated; see Volkwein et al. (2004) for more details on CPDMs. The CPDM was operated for the entire sampling time for these samples, and the air inlet to the instrument was positioned just adjacent to the air inlet for the dust sampling unit described above. A CPDM was not available when samples A4-A7 were collected, and the CPDM data at the *Miner* location (sample A11) was not obtained due to limited space, which prohibited consistent side-by-side positioning of the CPDM and dust sampling unit at that specific location.

The influence of large dust particles on dust characterization was also investigated for Data Set A, with the purpose of understanding if or how the presence of very large particles in a sample may affect apparent particle distributions. For this purpose, ten particles with  $L > 10 \mu\text{m}$  on each Data Set A sample were selected and characterized using a similar methodology to that used for characterization of the 100 particles used for comparative analysis between all samples. For the large particles, the SEM-EDX was operated at 2,500x magnification and particles were selected from the entire field of view, rather than from a limited area within the field as described in Chapter 2.

#### **4. Results and Discussion**

The dust characterization results for all samples are presented in Figures 3.1 and 3.3-3.5, which show filter particle densities, as well as composition, size and angularity distributions by number of particles, respectively. Results are presented as percent of total particles characterized per sample, and the 21 samples are grouped by similar sampling location (i.e., *Intake, Belt, Feeder, Return, Tram, Bolter, or Miner*) to allow comparisons between like locations.

Particle density, which was normalized by sampling time, was approximated from the filter area required to select 100 particles for SEM-EDX characterization using the methodology described above. From Figure 3.1, it appears that particle density is relatively similar between samples taken in the intake (i.e., all exhibit relatively low particle density) and near the feeder breaker (i.e., all exhibit moderate density). However, other location groups showed significant variation, and several samples exhibited very high apparent densities (i.e., A5, B4, and A10).

While filters were not analyzed gravimetrically (i.e., to determine the total mass of dust collected), observations from SEM work did indicate that particle deposition was relatively uniform on most samples.

Figure 3.1 additionally displays particle densities approximated from a particle counting routine that was completed on most of the filter subsections prepared for SEM-EDX analysis (i.e., 17 of the 21). The routine was done by counting the number of particles (with  $L > 0.5 \mu\text{m}$ ) observed on four different areas; each area was  $10,000 \mu\text{m}^2$  and located on a different quadrant of the filter subsection. The counting results are shown as average particle density observed between the four analyzed areas, again normalized by sampling time, and the error bars represent the 95% confidence interval. Results indicate that densities using the 100 particle estimation and densities by counting particles were remarkably similar. Moreover, for all but two samples (A1 and B5), the error bars on the particle counting-derived densities indicate that particles were indeed deposited relatively uniformly on the filter subsections taken for analysis. Figure 3.2 shows four example SEM images taken during the particle counting routine. While the A8 and A10 samples show relatively large numbers of particles, the much smaller number of particles on the A1 sample is clearly evident, which likely contributed to the wide error bars in Figure 3.1. Further, agglomerated particles were observed in several areas on sample B5, which certainly contributed to the variation in particle densities on the four areas analyzed during the counting routine. It is notable that particle agglomeration was not observed on any other sample; in the B5 sample, this may have been due to humidity in the intake air or the suspension of relatively wet particles by the movement of the mantrip.

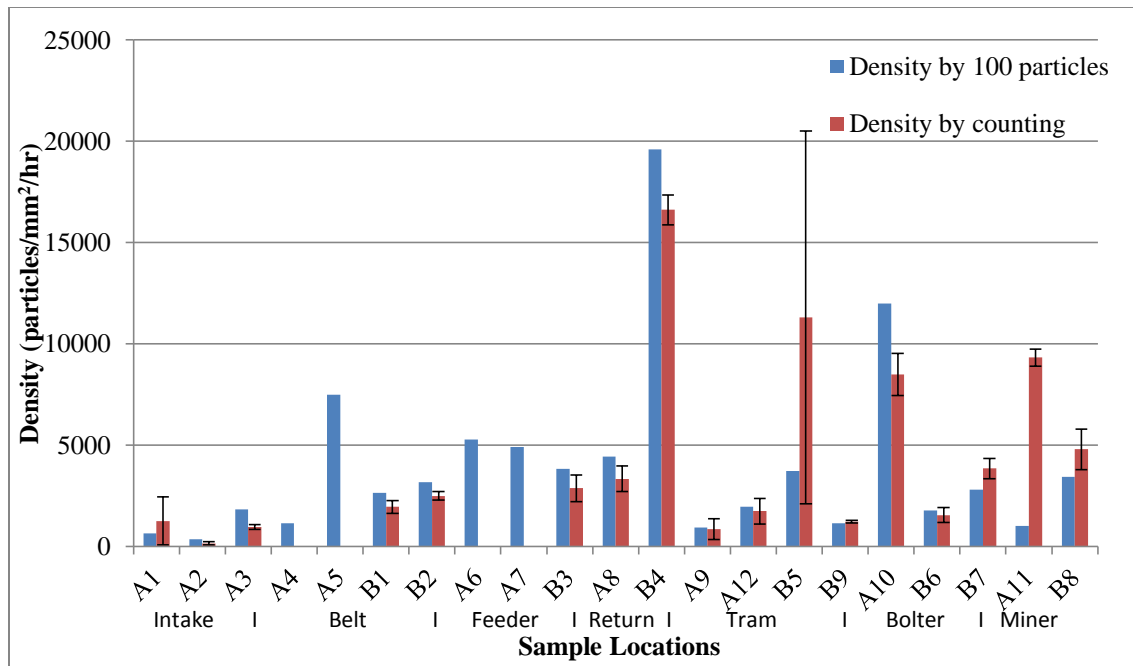


Figure 3.1. Approximated particle densities on each filter subsection. Densities were determined by two methods: using the area required to select 100 particles for SEM-EDX characterization and using the particle counting routine. Samples are grouped by similar sample locations.

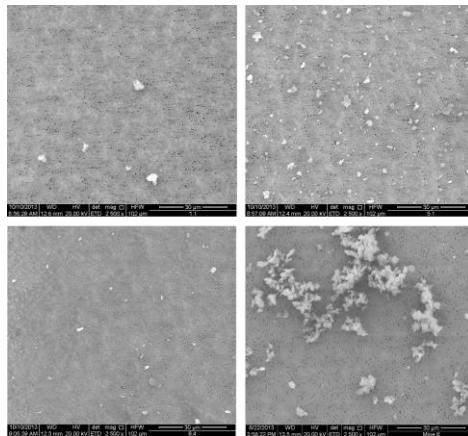


Figure 3.2. Clockwise from top left, SEM images of the A1, A10, B5, and A8 samples at 2,500x magnification.

In regards to compositional distributions, Figure 3.3 shows quite a bit of variation between samples in similar location groups, yet some trends are evident and possibly explainable. All *Intake* samples had > 30% carbonaceous (i.e., coal) dust, with small proportions of mixed carbonaceous particles compared to other groups. The *Tram* samples, which were also taken in intake air, had moderate proportions of carbonaceous particles but much higher proportions of carbonate particles, likely from rock dust kicked up by the moving mantrip. Carbonate

proportions were also elevated in the *Miner* and *Belt* samples, which again may be attributable to rock dusting in these areas.

The *Belt* and *Feeder* samples had high proportions of carbonaceous particles, which were expected since run-of-mine coal material is being disturbed in these areas. The relatively low carbonaceous particle numbers in the *Miner* operator samples might be explained by effective water sprays at the cutting face, which were positioned directly at the coal seam. Likewise, the low carbonaceous particle numbers in the *Bolter* operator samples may be attributed to the fact that the bolter was drilling into the roof rock, which is primarily shale, not coal. Indeed, the summed proportions of alumino-silicate and mixed carbonaceous particles were highest in the bolter samples as compared to all other sample groups; and, as discussed below, the particles classified as mixed carbonaceous are likely dominated by alumino-silicates that are very thin (i.e., small *S* dimension), biogenic (i.e., having some organic carbon content), or coated with ultrafine coal dust. The variation in the *Return* samples may be due to a number of factors, including different conditions in the working section during sampling (e.g., production rate, equipment positioning, etc.)

In terms of sample groups, the *Miner*, *Bolter*, and *Return* samples had the highest proportions of quartz particles (6-12% by number), although quartz was also high in several isolated samples in other groups; the B5 tramming sample actually had the highest number of quartz particles of all samples (14%). The relatively high number of unidentified particles (i.e., placed into the “other” compositional category) in the B3 feeder sample is possibly related to welding activities in this area during sample collection. No discernable trends were found in regards to heavy minerals between sample groups. However, anecdotally it should be noted that the EDX spectra across all samples indicated that many of the heavy mineral particles were likely metal oxides (e.g.,  $\text{TiO}_2$ ) rather than metal sulfides (e.g.,  $\text{FeS}_2$ ) as may often be expected in underground coal mines. This observation is consistent with the fact that the study mine produces metallurgical-grade coal, which is generally low in sulfur.

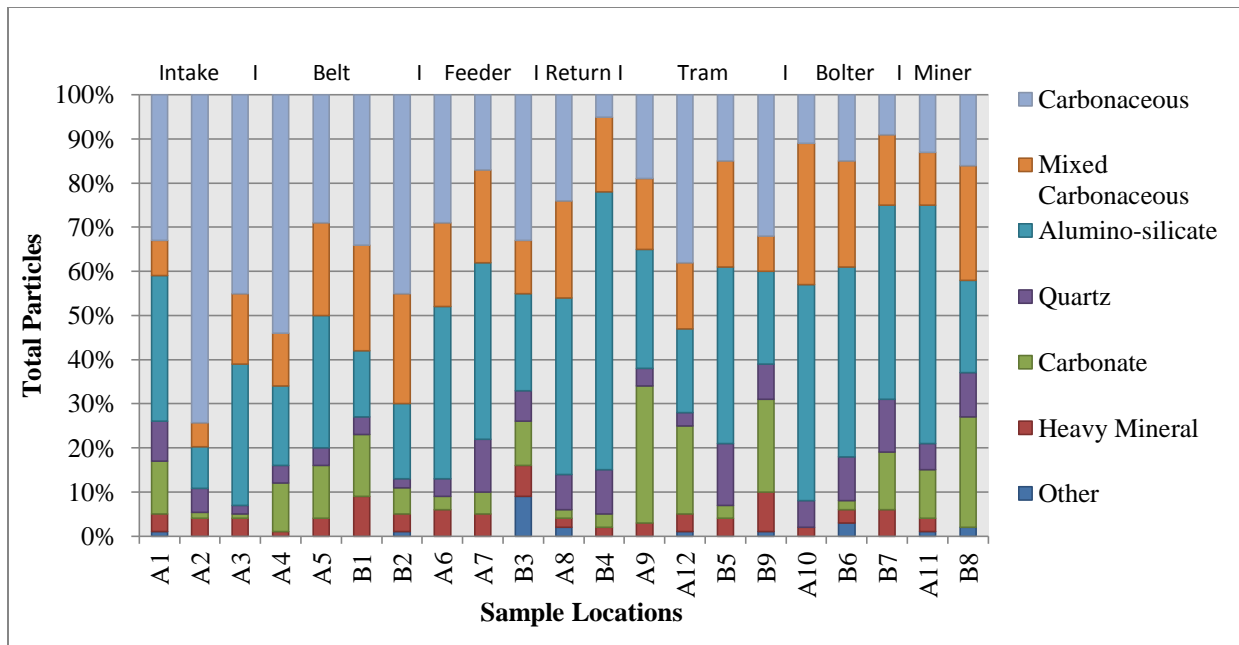


Figure 3.3. Composition distributions by number of particles for all twenty-one respirable dust samples. Samples are grouped by similar sample locations.

Figure 3.4 shows the particle size distribution in terms of spherical diameter for all 21 samples. Overall, most particles fell into the 0.5-1.0  $\mu\text{m}$ , 1.0-2.0  $\mu\text{m}$ , or 2.0-4.0  $\mu\text{m}$  size range. The *Bolter and Return* samples generally had smaller size distributions than other samples, consistent with the fact that material is actively being cut near the bolter operator and at the working face just upstream of the return sampling location. The fact that the size distribution was not particularly small near the miner operator could mean that dust control (e.g., water sprays and ventilation) were working well to keep freshly cut material away from the operator. In the *Intake* samples, the particle size distribution was relatively wide; but again, the *Tram* samples differed from the *Intake* samples somewhat, having fewer small particles (i.e., < 1  $\mu\text{m}$ ).

While characterization was only performed on particles with  $L > 0.5 \mu\text{m}$ , smaller particles were often observed on the sample filters. Given that coal is softer than the surrounding rock in the mine, it is believed that many of these particles were likely coal – though no attempt was made to conclusively determine their composition. Based on the current understanding of particle respiration and subsequent deposition in lung tissue (i.e., highest deposition for particles in the 1-2  $\mu\text{m}$  range), the particles included in the characterization methodology are indeed of the highest

concern; but future efforts will be focused on gaining some insights into smaller particle fractions as well.

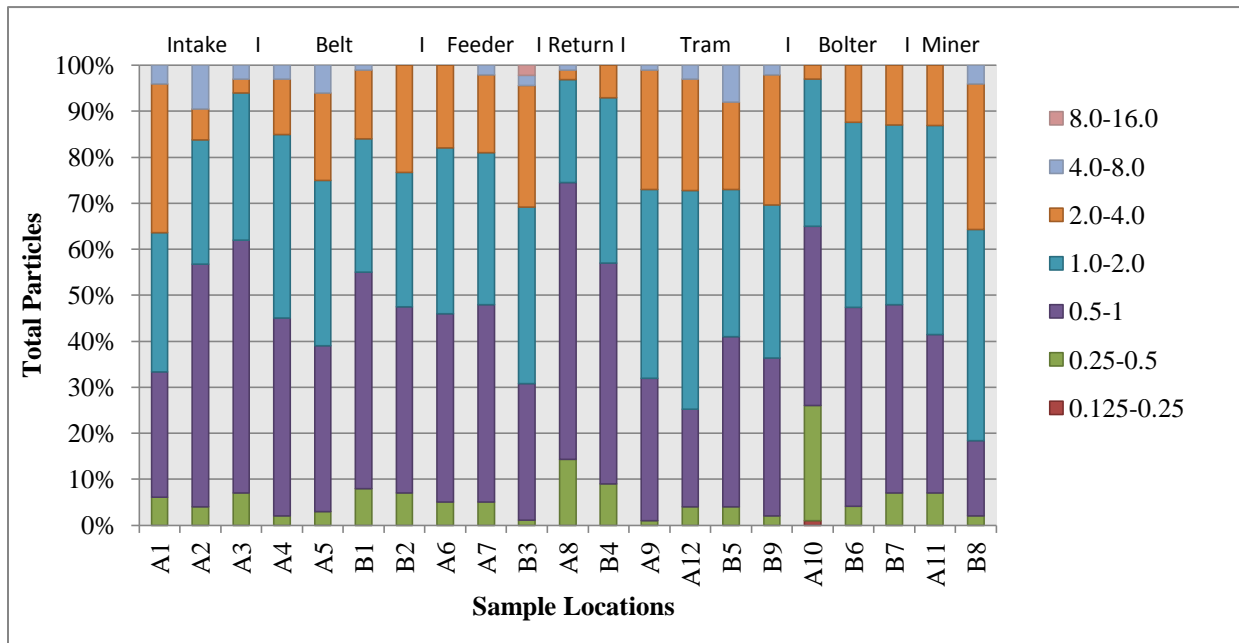


Figure 3.4. Size distributions by number of particles for all respirable dust samples, grouped by similar sample location. Size categories are based on each particles spherical diameter ( $\mu\text{m}$ ).

All but two of the dust samples (i.e., A5 and A10) were qualitatively assessed for angularity (Figure 3.5). Higher resolution is needed for a more accurate angularity assessment, therefore requiring a more in depth analysis. Overall, the majority of particles were found to be angular, with fewer particles being classified as transitional, and even fewer classified as rounded. While few trends could be discerned between samples grouped by location, the qualitative angularity assessments were useful in understanding more about the compositional categories. As illustrated by Figure 3.6, shape distributions were significantly different between these categories when compared across all samples. The carbonate, quartz and heavy mineral categories had similar numbers of angular and transitional particles, with very few rounded particles. Particles in all of these categories were commonly spherical in shape, and also somewhat larger in size, on average, than carbonaceous, alumino-silicate or mixed carbonaceous particles (Figure 3.7). The alumino-silicate, mixed carbonaceous and carbonaceous categories all exhibited high numbers of angular particles, but the relative proportion of the angular to transitional particles varied

substantially. For alumino-silicates, there were about 3.7x more angular particles than transitional, and about 3.8x more transitional particles than rounded. For the mixed carbonaceous category, these proportions were about 2.5x and 3.5x, respectively; and for the carbonaceous category, they were about 1.5x and 2.3x, respectively. Alumino-silicate particles, which likely originated from shale rock in these samples, are often highly angular due to the platy or sheet-like nature of the mineral grains. On the other hand, carbonaceous particles tend to fracture on smooth planes (Chirone and Massimilla, 1989), which could explain the higher proportions of transitional and rounded particles in this category. As shown in Table 3.2, particles classified into the mixed carbonaceous category have EDX spectra that exhibit both high aluminum and silicon peaks, characteristic of alumino-silicates, and high carbon peaks, characteristic of carbonaceous particles. Overall, the distribution of particle angularity for this category is more similar to that of the alumino-silicates (vs. the carbonaceous particles), which is consistent with prior work by the authors that found that mixed carbonaceous particles are often likely alumino-silicates that are thin enough to allow significant electron penetration during EDX analysis (i.e., false carbon peaks due to the PC filter media, as discussed by Laskin and Cowin, 2001), biogenic in nature, or coated with ultrafine coal dust (see Chapter 2).

While the actual composition of the mixed carbonaceous particles has not been conclusively determined, the particle size distributions shown Figure 3.7 provide further evidence to support the notion these particles are likely dominated by alumino-silicates. The figure includes three trend lines for this category, which vary due to the assumed *S:I* ratio value: the “carbonaceous like” line assumes ratio for these particles is the same as for carbonaceous particles (i.e., 0.6), the “alumino-silicate like” line assumes the ratio is the same as for the alumino-silicate particles (i.e., 0.4), and the “intermediate” line assumes the ratio is between the carbonaceous and alumino-silicate categories (i.e., 0.5). By assuming that the mixed carbonaceous particles are “alumino-silicate like,” the size distribution for these particles appears to be similar to both the alumino-silicate and carbonaceous particles; whereas either of the other assumptions results in a distribution with significantly larger particles – which seems quite implausible based on the measured dimensions (i.e., *L* and *I*, not shown) and visual observations during SEM work.

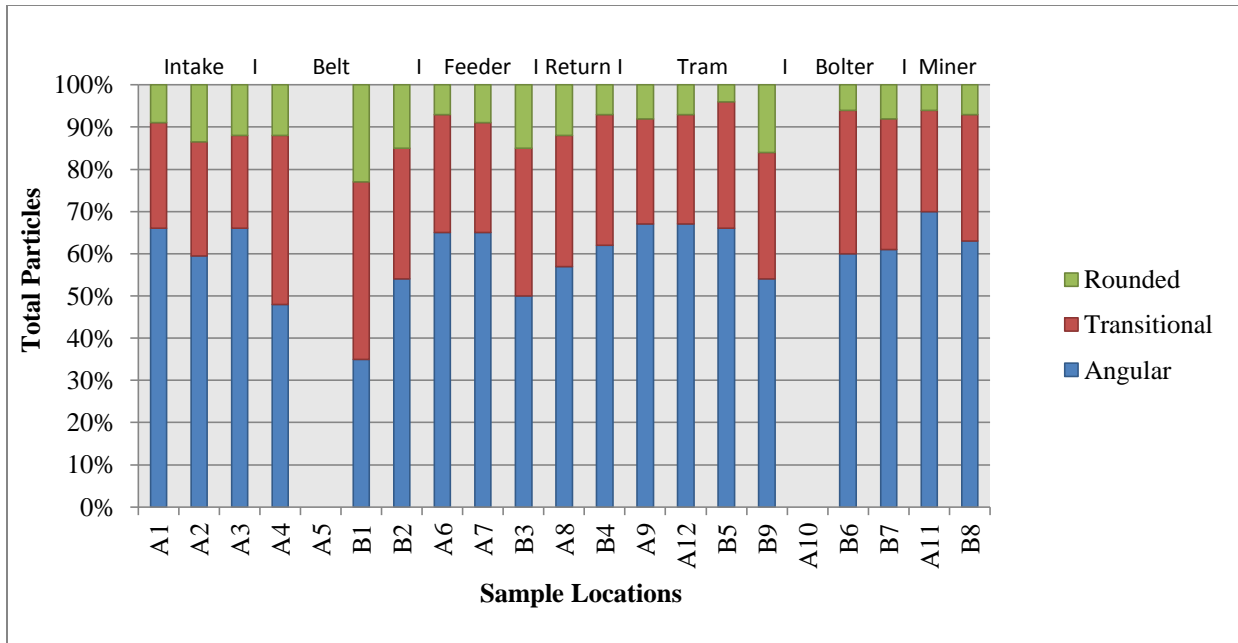


Figure 3.5. Qualitative shape distributions by number of particles for each sample, grouped by similar sample location. A5 and A10 samples were not characterized by shape.

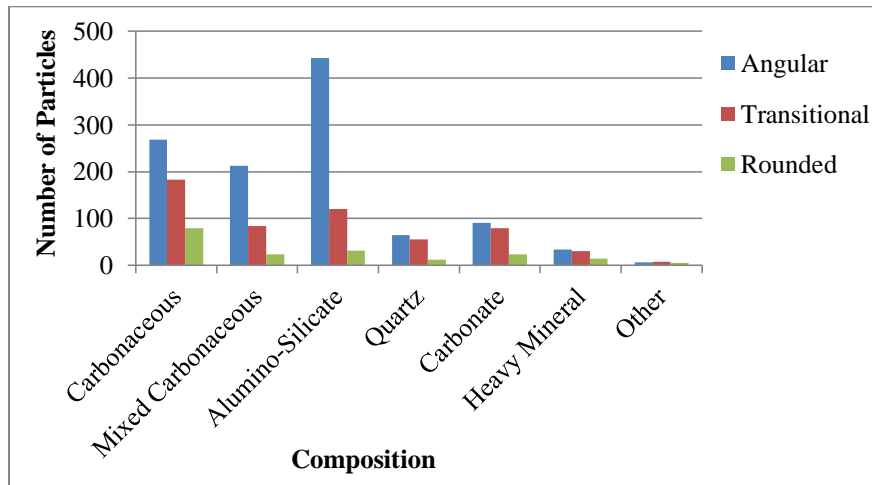


Figure 3.6. Shape distributions by number for each compositional category.

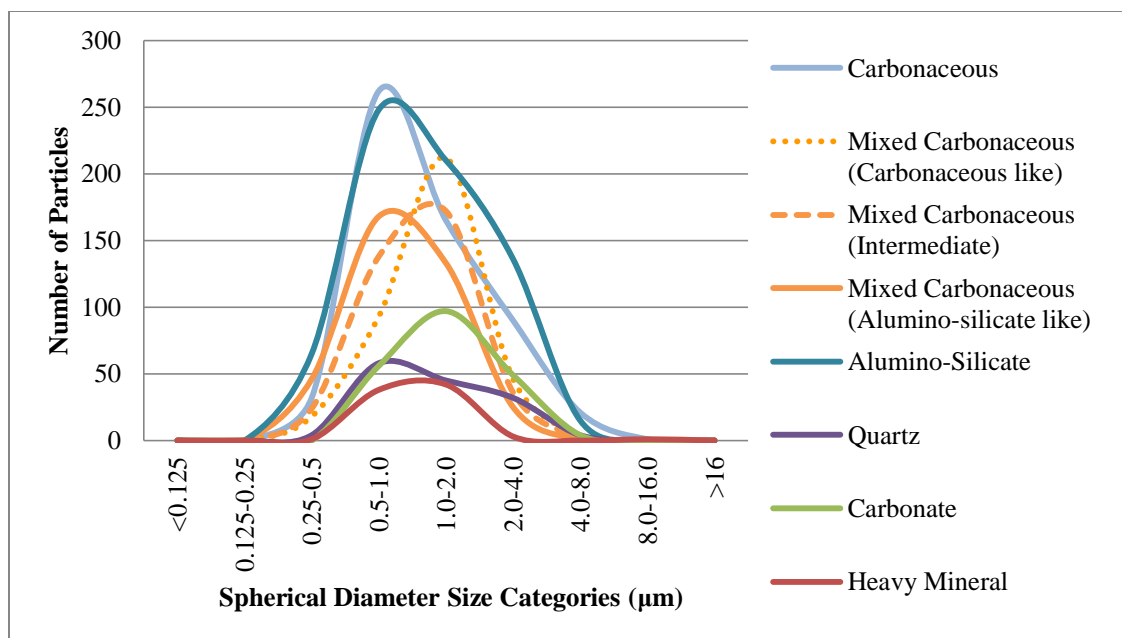


Figure 3.7. Size distributions by number for each compositional category.

For seven samples in Data Set A, CPDM data were used to determine the overall average respirable dust concentration ( $\text{mg}/\text{m}^3$ ) during sample collection. Figure 3.8 displays results comparing the CPDM-derived values to concentrations estimated from the particle distributions observed on each sample by SEM-EDX analysis. For this, the mass of each of the 100 particles characterized was estimated (i.e., by Equation 3.3), and the mass of these particles was extrapolated across the entire filter area based on the area of analysis needed to characterize 100 particles, the flow rate of the sampling pump, and the sampling time. Based on the above discussion, the mass of mixed carbonaceous particles was calculated using the SG for alumino silicates; however this assumption does not make a significant difference in the resulting concentration estimates. Results show that there appears to be a slight positive correlation between the CPDM-derived and estimated concentrations, but there are instances where the dust characterization results both over- and under-estimate the valued CPDM measurements.

Locations A8 and A10, which are *Return* and *Bolter* samples respectively, had relatively high CPDM concentrations consistent with the expected increase in respirable dust concentrations around these locations of the mine due to rock and coal cutting; however the estimated mass concentrations were much lower than expected. Throughout the SEM analysis of sample A8, it was observed that many small particles (i.e.,  $< 0.5 \mu\text{m}$  in size) were collected on the filter. As

stated above, due to the characterization procedure, these particles are left uncharacterized. This may not only influence the composition distribution but also the filter particle density. If large quantities of small particles are present in the air, CPDM mass would be increased as well as particle density, yet the procedure is not taking into account the mass of all these small particles. Also, by only analyzing larger particles, the calculated filter particle density (4,444 particles/mm<sup>2</sup>) is lower than the actual particle density and therefore the mass is underestimated as a result.

Sample A10 had a much higher calculated particle density (11,981 particles/mm<sup>2</sup>), yet the estimated mass concentration was still much lower than the CPDM value. The reason for this discrepancy may be linked to particle size. Because only a small area of the filter needed to be analyzed to capture 100 particles, it is possible that fewer particles with  $d_s > 2.0 \mu\text{m}$  were characterized, as larger particles occur less frequently on the filters. Only 9% of the analyzed particles in this sample had  $d_s > 2.0 \mu\text{m}$ , which is much smaller than the average size distribution of larger particles for most of the samples. The mass of the smaller, characterized particles may underestimate the actual mass of particles collected on the filter, since larger particles contribute more to mass. It is likely that larger particles do exist on sample A10, but remain uncharacterized.

In contrast to sample A10, sample A12 had a higher than expected estimated mass concentration compared to the CPDM value, which may be due to a lower density sample and the characterization of larger particles. When comparing the raw size distribution data for this sample, there were significantly more particles in larger size ranges than many of the other samples. It is known that 2-piece cassettes cause larger particles to be deposited near the center of the filter (Baron, 2003); therefore the mass may be overestimated by only analyzing the center 9 mm filter area and extrapolating the mass to the entire 37 mm filter.

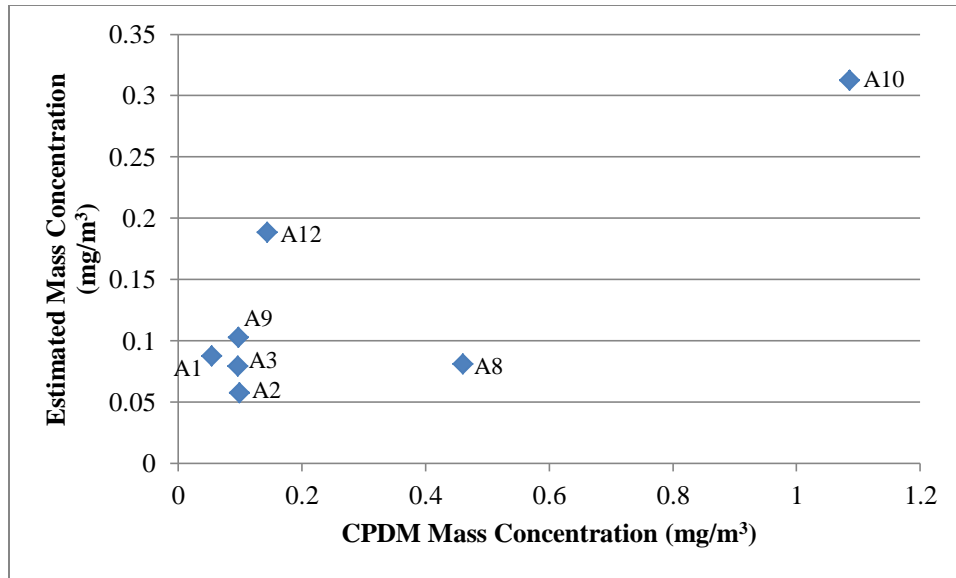


Figure 3.8. Estimated mass concentrations and average CPDM mass concentrations for seven Data Set A samples.

Although less common, large particles outside the respirable range may be collected on sample filters, even with the use of a cyclone. Practically, this is important since the mass of such particles may significantly influence analyses to determine total respirable dust concentration, and also crystalline silica content. Table 3.3 displays the results of characterizing a maximum of ten large dust particles (i.e.,  $L > 10 \mu\text{m}$ ) for all Data Set A samples. The large particles were characterized by composition, and the total filter subsection area required to select ten particles for analysis based on the method previously described was determined. Across all samples (i.e., 110 total particles), approximately two-thirds of the large particles characterized were carbonaceous and approximately one-third were alumino-silicates. Only a few particles were classified into the remaining compositional categories, and notably only one of particles was classified as mixed carbonaceous. This result further suggests that many of the smaller mixed carbonaceous particles included in the respirable-sized dust analysis (i.e., where they comprised 4-32% of all characterized particles in each sample) may indeed be alumino-silicates that were prone to electron penetration.

*Table 3.3 Compositional distributions by number large dust particles observed on Data Set A samples.*

| Data Set A    | Carbon.   | Mixed Carbon. | Alumino-Silicate | Quartz   | Carbonate | Heavy Mineral | Other    | Total Area of Analysis (mm <sup>2</sup> ) | Estimated Area of Analysis for 30 Particles (mm <sup>2</sup> ) |
|---------------|-----------|---------------|------------------|----------|-----------|---------------|----------|---|--|
| A1            | 7         | 0             | 3                | 0        | 0         | 0             | 0        | 2.23                                      | 6.69   |
| A2            | 8         | 0             | 2                | 0        | 0         | 0             | 0        | 1.71                                      | 5.13   |
| A3            | 9         | 0             | 1                | 0        | 0         | 0             | 0        | 1.41                                      | 4.22   |
| A4            | 8         | 0             | 2                | 0        | 0         | 0             | 0        | 0.46                                      | 1.39   |
| A5            | 7         | 0             | 3                | 0        | 0         | 0             | 0        | 1.47                                      | 4.42   |
| A6            | 1         | 0             | 1                | 0        | 0         | 0             | 0        | 4.54                                      | 68.07  |
| A7            | 5         | 0             | 3                | 0        | 1         | 1             | 0        | 2.34                                      | 7.01   |
| A8            | 2         | 1             | 2                | 0        | 3         | 0             | 0        | 4.46                                      | 16.71  |
| A9            | 3         | 0             | 6                | 1        | 0         | 0             | 0        | 1.46                                      | 4.37   |
| A10           | 6         | 0             | 1                | 1        | 1         | 1             | 0        | 2.61                                      | 7.84   |
| A11           | 8         | 0             | 2                | 0        | 0         | 0             | 0        | 0.24                                      | 0.73   |
| A12           | 3         | 0             | 6                | 0        | 1         | 0             | 0        | 2.83                                      | 8.49   |
| <b>Totals</b> | <b>67</b> | <b>1</b>      | <b>32</b>        | <b>2</b> | <b>6</b>  | <b>2</b>      | <b>0</b> | -   | -  |

The required area for the large particle analysis was also extrapolated to estimate the filter area that would have been required to characterize 30 particles. The reason for doing this is that, when operator samples are collected to demonstrate compliance with dust regulations, a sample is discarded if 30 or more large particles are found within a 2.5 mm<sup>2</sup> area on the filter (Volkwein, 2008). The results shown in Table 3.3 indicate that, For ten of the twelve samples, it was estimated that more than 2.5 mm<sup>2</sup> of the filter would need to be analyzed in order to characterize 30 large particles; however samples A4 and A11 did not meet this criterion since an area of only 1.39 and 0.73 mm<sup>2</sup>, respectively, was estimated for analysis of 30 large particles. As such, these samples would have likely been discarded had they been collected for regulatory compliance purposes. The mass of these large particles would not only overestimate the respirable dust concentration associated with the samples, but would also increase the associated mass percentage of carbonaceous dust – and thus decrease the mass percentage of other dust components such as silica.

## 5. Conclusions

While only a limited number of samples were collected from a single study mine, the results presented here show that respirable dust composition, size and shape, can vary widely within an underground coal mine. Routine particle-level characterization of mine dusts would represent a particularly significant advancement, and exploration of analytical techniques is imperative for developing effective and efficient methodologies. This paper has demonstrated several basic utilities of SEM-EDX for coal mine dusts, and much more is certainly possible – particularly in view of the potential for computer automated analysis, which would make feasible the characterization of relatively many more particles per sample. In the current work, a relatively small number of particles per sample could be characterized, and some of challenges related to extrapolation of results across an entire sample were highlighted. The presence of relatively small particles that exhibit EDX spectra characteristics expected for both coal and specific mineral particles is also a challenge. In the context of occupational health, dust analysis methodologies that include both bulk and particle-level characteristics would be ideal.

## 6. Acknowledgements

The authors would like to thank the study mine employees that assisted in the dust sample collection process. We would also like to thank VT NCFL and Steve McCartney for operational assistance with SEM.

## 7. References

- American Conference of Governmental Industrial Hygienis (ACGIH) (2005). *TLVs and BEIs: Based on the documentation of the threshold limit values for chemical substances and physical agents and biological exposure indices*. Cincinnati, OH.
- Attfield, M., Hale, J., et al. (2011). Current Intelligence Bulletin 64: Coal Mine Dust Exposures and Associated Health Outcomes – A Review of Information Published Since 1995. DHHS (NIOSH), Publication No. 2011-172.

Attfield, M., Seixas, N. (2007). Prevalence of pneumoconiosis and its relationship to dust exposure in a cohort of U.S. Bituminous coal miners and ex-miners. *American Journal of Independent Medicine*, 27(1), 137-51.

Baron, P. (2003). Factors Affecting Aerosol Sampling, NIOSH Manual of Analytical Methods. *NIOSH/DART, O*, 184-207.

Bruker (2014). Bruker Corporation, Ewing, NJ: Bruker Corp.

Centers for Disease Control (CDC) (2006). Advanced Cases of Coal Workers' Pneumoconiosis- Two Counties, Virginia. *MMWR*, 55(33).

Centers for Disease Control (CDC) (2012). Pneumoconiosis and Advanced Occupational Lung Disease Among Surface Coal Miners – 16 States, 2010-2011. *MMWR*, 61(23), 431-434.

Chirone, R., Massimilla, L. (1989). Primary fragmentation of a coal in fluidized bed combustion. *Symposium (International) on Combustion*, 2(1), 267-277.

Coal Workers' Health Surveillance Program (CWHSP) Data Query System (2014). Occupational Respiratory Disease Surveillance, Available at: <http://webappa.cdc.gov/ords/cwhsp-database.html>.

Courtney, W., Cheng, L., Divers, E. (1986). Deposition of Respirable Coal Dust in an Airway. *US Bureau of Mines, Report of Investigations*, RI 9041.

Dullea E., Chajet, H. (2013). *Is MSHA About to Defy Science, Logic & Law with a New Coal Dust Rule?*. *Coal Age*, 72.

EPA (1999). Air quality criteria for particulate matter (Vol. II). Technical Report, EPA document 600/P-99/002bEPA.

Federal Coal Mine Health and Safety (CMHSA) Act (1969). Public Law No. 91-173.

Federal Register (2010). Lowering Miner's Exposure to Respirable Coal Mine Dust, Including Continuous Personal Dust Monitors; Proposed Rule, *75 Fed. Reg.* 64412.

Federal Register (2014). Lowering Miner's Exposure to Respirable Coal Mine Dust, Including Continuous Personal Dust Monitors; Final Rule, *79 Fed. Reg.* 24813.

FEI (2014). FEI Company, Hillsboro, OR: FEI Corp.

Gamble, J., Reger, R., Glenn, R. (2011). Rapidly progressing coal workers pneumoconiosis as a confounding risk factor in assessing coal mine dust safe exposure levels. *Journal of Clinical Toxicology*, S:1-003.

- Hassan, M., Lau, R. (2009). Effect of particle shape on dry particle inhalation: study of flowability, aerosolization, and deposition properties. *AAPS PharmSciTech*, 10(4), 1252-1262.
- ISO (1995). *Air quality-particle size fraction definitions for health related sampling*, ISO Standard 7708. International Organization for Standardization (ISO), Geneva.
- Landen, D., Wassel, A., McWilliams, L., Patel, J. (2011). Coal dust exposure and mortality from ischemic heart disease among a cohort of U.S. coal miners. *American Journal of Industrial Medicine*, 54(10), 727-733.
- Laney, A. S., Petsonk, E., Hale, J., et al. (2012). Potential determinants of coal workers' pneumoconiosis, advanced pneumoconiosis, and progressive massive fibrosis among underground coal miners in the United States, 2005-2009. *American Journal of Public Health*, 102(S2), S279-S283.
- Laney, A., Attfield, M. (2014). Examination of Potential Sources of Bias in the US Coal Workers' Health Surveillance Program. *American Journal of Public Health*, 104(1), 165-170.
- Laney, S., Petsonk, E., Attfield, M. (2010). Pneumoconiosis among underground bituminous coal miners in the United States: is silicosis becoming more frequent?. *Occupational Environmental Medicine*, 67, 652-656.
- Laskin, A., Cowin, J. (2001). Automated Single-Particle SEM/EDX Analysis of Submicron Particles down to 0.1  $\mu\text{m}$ . *Analytical Chemistry*, 73, 1023-1029.
- Liebhard, M., Levy, A. (1991). The effect of erodent particle characteristics on the erosion of metals. *Wear*, 151(2), 381-390.
- Maher, K. (2014). *Coal Industry Asks Court to Review New Coal Dust Rules*. The Wall Street Journal.
- National Institute for Occupational Safety and Health (NIOSH) (2003). The 2002 Work-related Lung Disease Surveillance Report. *NIOSH*, Cincinnati, OH.
- Page, S., Organiscak, J. (2002). Using proximate analysis to characterize airborne dust generation from bituminous coals. *Aerosol Science and Technology*, 36(6), 721-733.
- Pollock, D., Potts, J., Joy, G. (2010). Investigation into dust exposures and mining practices in mines in the southern Appalachian region. *Mining Engineering*, 62(2), 44-49.
- Respirable Dust Standard when Quartz is Present, 30 CFR Part 70.101, (1994).

- Ross, M., Murray, J. (2004). Occupational respiratory disease in mining. *Occupational Medicine*, 54(5), 304-310.
- Santo Tomas, L. (2011). Emphysema and chronic obstructive pulmonary disease in coal miners. *Current Opinion in Pulmonary Medicine*, 17(2), 123-125.
- Sneed, E., Folk, R. (1958). Pebbles in the Lower Colorado River, Texas, a study in particle morphogenesis. *The Journal of Geology*, 6(2), 114-150.
- Stachowiak, G. (1998). Numerical Characterization of Wear Particles Morphology and Angularity of Particles and Surfaces. *Tribology International*, 31(1-3), 139-157.
- Suarthana, E., Laney, A., Storey, E., et al. (2011). Coal workers' pneumoconiosis in the United States: regional differences 40 years after implementation of the 1969 Federal Coal Mine Health and Safety Act. *Occupational Environmental Medicine*, 68, 908–913.
- Volkwein, J. (2008). Analysis of particulate contamination in personal dust monitor sampling. Proceedings of the 12th U.S./North American Mine Ventilation Symposium, Reno, Nevada, June 9-11, 2008, 353-358.
- Volkwein, J., et al. (2004). Performance of a New Personal Respirable Dust Monitor for Mine Use. U.S. Department of Health and Human Services, CDC, *Report of Investigations*, RI 9663, Pittsburgh, PA.
- Weber, C., Heuser, M., Mertens, G., Stanjek, H. (2014). Determination of clay mineral aspect ratios from conductive titrations. *Clay Minerals*, 49(1), 17-26.
- WHO (1997). Silica, Some Silicates, Coal Dust and Para-aramid Fibrils. World Health Organization (WHO), International Agency for Research on Cancer (IARC), 68.
- WHO (1999). Hazard Prevention and Control in the Work Environment: Airborne Dust, World Health Organization (WHO), Occupational and Environmental Health: Department of Protection of the Human Environment, Geneva, 99.

## CHAPTER 4: CONCLUSIONS AND FUTURE WORK

This purpose of this project was to determine the usefulness of a more comprehensive respirable dust characterization protocol for coal mines. A standard method was developed using scanning electron microscopy with energy dispersive x-ray (SEM-EDX) for particle level analysis of dust generally < 10 µm in size. Small scale experiments were conducted using lab generated dust to determine the mineralogy of coal mine dust, from a specific mine in Central Appalachia, and particle characteristics of interest. A detailed method was developed to unbiasedly and efficiently select particles to characterize using SEM images and EDX spectra analysis. The method was verified and demonstrated using respirable dust samples collected from the same underground mine in Central Appalachia. Samples were characterized by composition, size, shape, and mass distributions. The developed characterization protocol generated an abundance of data which allowed a more comprehensive analysis of respirable dust.

Although much progress was made for respirable dust analysis using SEM-EDX, future work is recommended as a result of this research.

### *Near Term Work*

1. The deposition uniformity of 2 or 3-piece cassettes should be explored, given that the analytical method outlined in this report only uses the 9 mm center sub-section of the 37 mm filter.
2. Possible changes should be made to the dust characterization method to ensure it is more universal and can be applied to common coal mine dusts of various mines and locations.
3. The analysis should be completed by various users with the same samples, to confirm that results can be replicated
4. Work should also be completed to further explore the origin of “mixed carbonaceous” dust so that electron penetration or fine coal dust does not influence the classification alumino-silicate particles.

### *Long Term Work*

1. Respirable dust samples should be collected from different coal mines and analyzed using the standard method, to further verify that the protocol is both efficient and can produce the important information pertaining to respirable dust exposures.

2. The influence of large particles on respirable mass concentrations should be investigated in terms of personal dust samples using the described method and CPDM samples.
3. Work should be done to investigate how the comprehensive data collected from the respirable dust samples may aid in understanding occupational health risks for coal mine workers.
4. After determining high risk occupations based on the exposure of hazardous dust, engineering work should be completed to help minimize these specific dusts from being generated in dangerous concentrations or becoming airborne whatsoever.

APPENDIX A: CHAPTER 2 SUPPLEMENTAL DATA

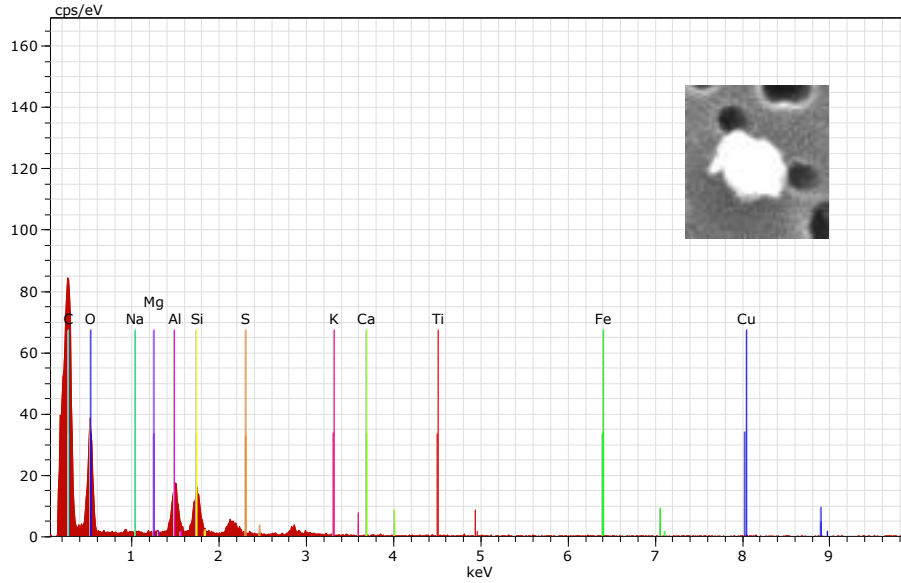


Figure A.1. Example of a particle classified as mixed carbonaceous.

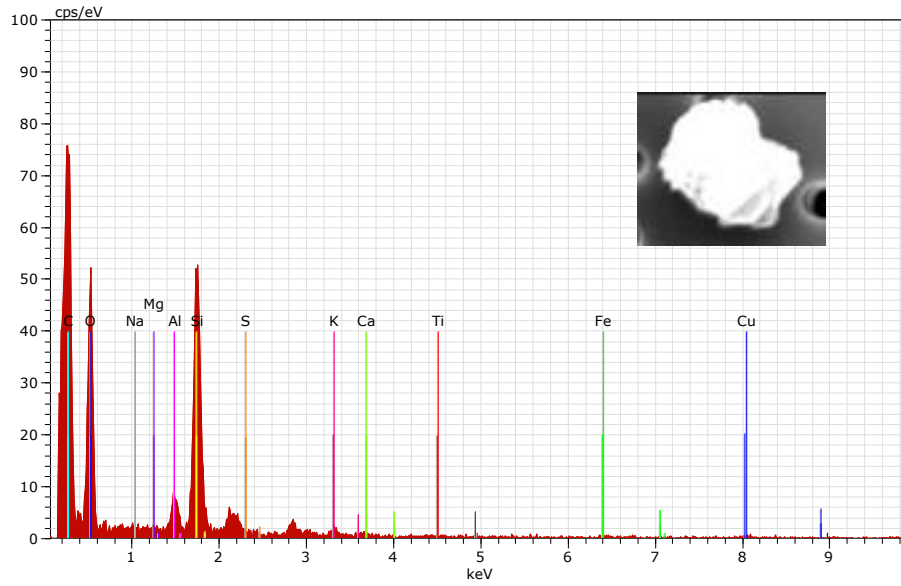
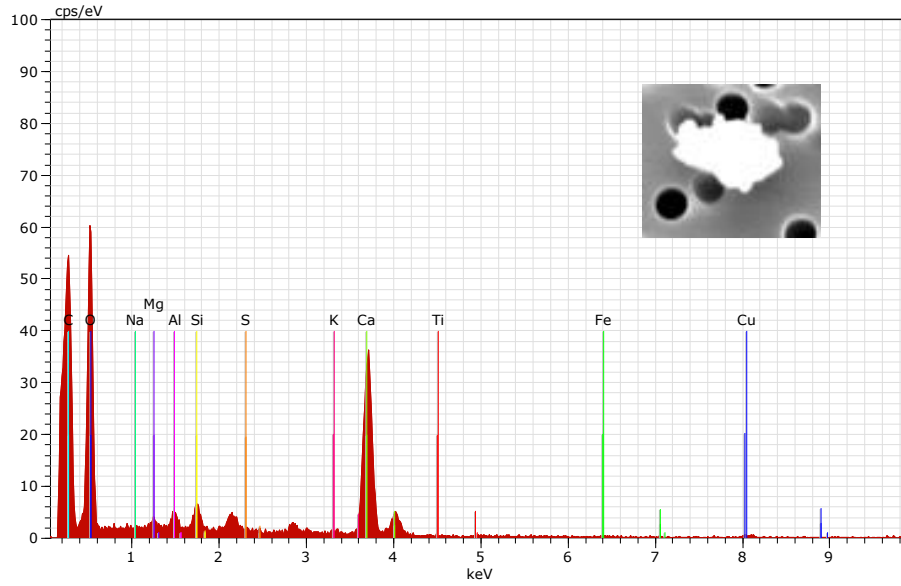
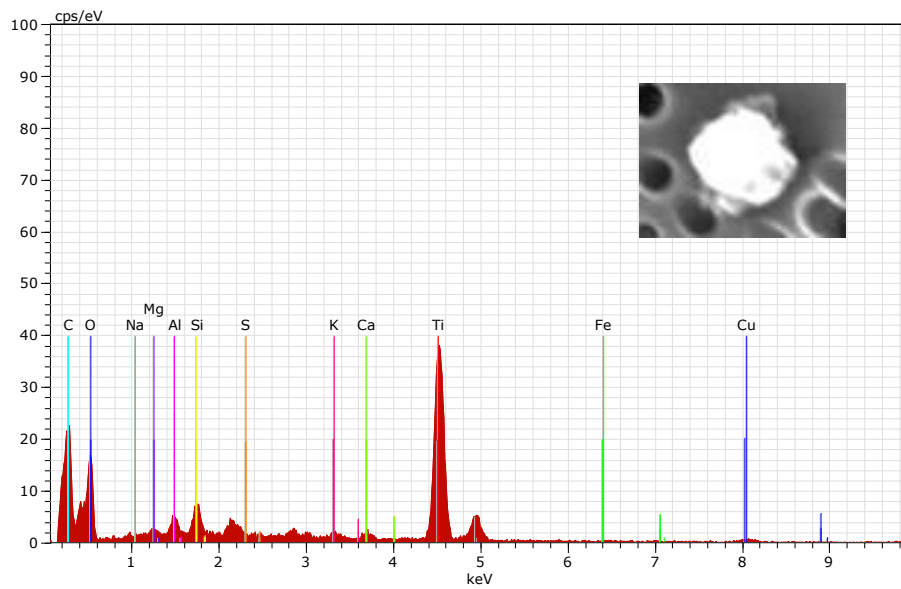


Figure A.2. Example of a particle classified as quartz.



*Figure A.3. Example of a particle classified as carbonate.*



*Figure A.4. Example of a particle classified as heavy mineral.*



| Spherical Diameter Size Distributions (# of Particles)       |    | <0.125   | 0.125-0.25 | 0.25-0.5 | 0.5-1.0  | 1.0-2.0  | 2.0-4.0  | 4.0-8.0  | 8.0-16.0 | >16.0    | Total    |
|--|----|----------|------------|----------|----------|----------|----------|----------|----------|----------|----------|
| Carbonaceous   | c  | 0        | 0          | 0        | 0        | 0        | 0        | 0        | 0        | 0        | 0        |
| Mixed Carbonaceous   | mc | 0        | 0          | 0        | 0        | 0        | 0        | 0        | 0        | 0        | 0        |
| Alumino-Silicate   | as | 0        | 0          | 0        | 0        | 0        | 0        | 0        | 0        | 0        | 0        |
| Quartz   | q  | 0        | 0          | 0        | 0        | 0        | 0        | 0        | 0        | 0        | 0        |
| Carbonate  | at | 0        | 0          | 0        | 0        | 0        | 0        | 0        | 0        | 0        | 0        |
| Heavy Mineral  | h  | 0        | 0          | 0        | 0        | 0        | 0        | 0        | 0        | 0        | 0        |
| Other  | o  | --       | --         | --       | --       | --       | --       | --       | --       | --       | --       |
| Cross-sectional Diameter Size Distributions (# of Particles) |    | <0.125   | 0.125-0.25 | 0.25-0.5 | 0.5-1.0  | 1.0-2.0  | 2.0-4.0  | 4.0-8.0  | 8.0-16.0 | >16.0    | Total    |
| Carbonaceous   | c  | 0        | 0          | 0        | 0        | 0        | 0        | 0        | 0        | 0        | 0        |
| Mixed Carbonaceous   | mc | 0        | 0          | 0        | 0        | 0        | 0        | 0        | 0        | 0        | 0        |
| Alumino-Silicate   | as | 0        | 0          | 0        | 0        | 0        | 0        | 0        | 0        | 0        | 0        |
| Quartz   | q  | 0        | 0          | 0        | 0        | 0        | 0        | 0        | 0        | 0        | 0        |
| Carbonate  | at | 0        | 0          | 0        | 0        | 0        | 0        | 0        | 0        | 0        | 0        |
| Heavy Mineral  | h  | 0        | 0          | 0        | 0        | 0        | 0        | 0        | 0        | 0        | 0        |
| Other  | o  | --       | --         | --       | --       | --       | --       | --       | --       | --       | --       |
| 0  |    |          |            |          |          |          |          |          |          |          |          |
| Spherical Diameter Size Distributions by Mass                |    | <0.125   | 0.125-0.25 | 0.25-0.5 | 0.5-1.0  | 1.0-2.0  | 2.0-4.0  | 4.0-8.0  | 8.0-16.0 | >16.0    | Total    |
| Carbonaceous   | c  | 0.00E+00 | 0.00E+00   | 0.00E+00 | 0.00E+00 | 0.00E+00 | 0.00E+00 | 0.00E+00 | 0.00E+00 | 0.00E+00 | 0.00E+00 |
| Mixed Carbonaceous   | mc | 0.00E+00 | 0.00E+00   | 0.00E+00 | 0.00E+00 | 0.00E+00 | 0.00E+00 | 0.00E+00 | 0.00E+00 | 0.00E+00 | 0.00E+00 |
| Alumino-Silicate   | as | 0.00E+00 | 0.00E+00   | 0.00E+00 | 0.00E+00 | 0.00E+00 | 0.00E+00 | 0.00E+00 | 0.00E+00 | 0.00E+00 | 0.00E+00 |
| Quartz   | q  | 0.00E+00 | 0.00E+00   | 0.00E+00 | 0.00E+00 | 0.00E+00 | 0.00E+00 | 0.00E+00 | 0.00E+00 | 0.00E+00 | 0.00E+00 |
| Carbonate  | at | 0.00E+00 | 0.00E+00   | 0.00E+00 | 0.00E+00 | 0.00E+00 | 0.00E+00 | 0.00E+00 | 0.00E+00 | 0.00E+00 | 0.00E+00 |
| Heavy Mineral  | h  | 0.00E+00 | 0.00E+00   | 0.00E+00 | 0.00E+00 | 0.00E+00 | 0.00E+00 | 0.00E+00 | 0.00E+00 | 0.00E+00 | 0.00E+00 |
| Other  | o  | --       | --         | --       | --       | --       | --       | --       | --       | --       | --       |
| 0.00E+00   |    |          |            |          |          |          |          |          |          |          |          |

Figure A.8. Automated analysis workbook size distribution output screen

| Dust Classification                              | ID | Total Mass (ug) | Percent of Total Mass (%) |
|--|----|-----------------|---------------------------|
| Carbonaceous                                     | c  | 0.0000E+00      | #DIV/0!                   |
| Mixed Carbonaceous                               | mc | 0.0000E+00      | #DIV/0!                   |
| Alumino-Silicate                                 | as | 0.0000E+00      | #DIV/0!                   |
| Quartz   | q  | 0.0000E+00      | #DIV/0!                   |
| Carbonate  | at | 0.0000E+00      | #DIV/0!                   |
| Heavy Mineral                                    | h  | 0.0000E+00      | #DIV/0!                   |
| <b>Total Measured (ug)</b>                       |    | 0.0000E+00      |                           |
| <b>Estimated on Sub-Section (ug)</b>             |    | 0               |                           |
| <b>Estimated on Whole Filter (ug)</b>            |    | 0               |                           |
| <b>Estimated Concentraion (mg/m<sup>3</sup>)</b> |    | #DIV/0!         |                           |

Figure A.9. Automated analysis workbook mass distribution output screen

| Angular a            |    |     |         | Transitional t            |    |     |         | Rounded r            |    |     |         |
|----------------------|----|-----|---------|---------------------------|----|-----|---------|----------------------|----|-----|---------|
| Dust Classification  | ID | No. | %       | Dust Classification       | ID | No. | %       | Dust Classification  | ID | No. | %       |
| Carbonaceous         | c  | 0   | #DIV/0! | Carbonaceous              | c  | 0   | #DIV/0! | Carbonaceous         | c  | 0   | #DIV/0! |
| Mixed Carbonaceous   | mc | 0   | #DIV/0! | Mixed Carbonaceous        | mc | 0   | #DIV/0! | Mixed Carbonaceous   | mc | 0   | #DIV/0! |
| Alumino-Silicate     | as | 0   | #DIV/0! | Alumino-Silicate          | as | 0   | #DIV/0! | Alumino-Silicate     | as | 0   | #DIV/0! |
| Quartz               | q  | 0   | #DIV/0! | Quartz                    | q  | 0   | #DIV/0! | Quartz               | q  | 0   | #DIV/0! |
| Carbonate            | at | 0   | #DIV/0! | Carbonate                 | at | 0   | #DIV/0! | Carbonate            | at | 0   | #DIV/0! |
| Heavy Mineral        | h  | 0   | #DIV/0! | Heavy Mineral             | h  | 0   | #DIV/0! | Heavy Mineral        | h  | 0   | #DIV/0! |
| Other                | o  | 0   | #DIV/0! | Other                     | o  | 0   | #DIV/0! | Other                | o  | 0   | #DIV/0! |
| <b>Total Angular</b> |    | 0   |         | <b>Total Transitional</b> |    | 0   |         | <b>Total Rounded</b> |    | 0   |         |

Figure A.10. Automated analysis workbook shape distribution output screen